

Impact of Surface Properties — Including Pore Size — of Porous Structures on Anticancer Drug Delivery Efficiency in Colon Cancer: A Systematic Review

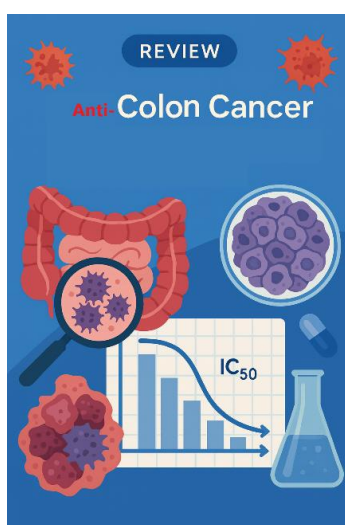
Sana Tat*^{ORCID}, Ehsan Mohebbi and Ali Reza Akbarzadeh

Department of Inorganic Chemistry, Iran University of Science and Technology, Tehran, Iran

***Corresponding Author**

Sana Tat, Department of Inorganic Chemistry, Iran University of Science and Technology, Tehran, Iran.

Submitted: 2026, Mar 03; Accepted: 2026, May 29; Published: 2026, Jun 15



Citation: Tat, S., Mohebbi, E., Akbarzadeh, A. R. (2026). Impact of Surface Properties — Including Pore Size — of Porous Structures on Anticancer Drug Delivery Efficiency in Colon Cancer: A Systematic Review. *Adv Hema Onco Res*, 9(2), 01-24.

Abstract

Porous materials with micro-, meso-, and macroporous structures receive increasing attention as multifunctional platforms for targeted drug delivery in colon cancer therapy. Their adjustable pore sizes, tunable surface chemistry, and adaptable structural frameworks enable controlled drug loading and release. Pore size distribution's impact on treatment efficacy is under-investigated. In line with PRISMA 2020 guidelines, this review systematically examined more than 3,000 studies and, based on performance criteria, identified 203 articles for inclusion. The IUPAC pore classification elucidates the impact of pore diameters on drug diffusion, cellular uptake, and cytotoxicity, highlighting their essential function in multi-modal treatment techniques.

Recent advancements in pH-responsive systems, aptamer-mediated targeting, and hierarchical porosity engineering illustrate how these integrated mechanisms augment site-specific drug delivery and enhance therapeutic selectivity. The review emphasizes essential design principles and future outlooks for creating next-generation porous carriers, whereby pore size, surface functionality, and biological responsiveness work in concert to enhance colon cancer therapy.

Keywords: PRISMA, IUPAC Pore Classification, Microporous Systems, Mesoporous Systems, Drug Delivery, Colon Cancer

1. Introduction

Porous drug-delivery platforms have become central to emerging therapeutic strategies for colon cancer due to their high surface area, tunable internal architecture, and capacity for

controlled drug loading and release [1]. In the past ten years, materials such as mesoporous silica, metal-organic frameworks, polymeric hydrogels, zeolites, and hybrid nanoarchitectures have demonstrated promising in-vitro performance. Nonetheless,

despite the variety of existing systems, a critical question persists: to what degree does pore size, independent of material chemistry, influence cytotoxic effects in colon cancer models? [2-7].

Most current evaluations classify porous systems according to material type or synthesis method, which complicates the assessment of mechanistic trends that transcend material categories [8]. The literature is deficient in a cohesive analytical framework based on the IUPAC pore-size classification (microporous <2 nm, mesoporous 2–50 nm, macroporous >50 nm) [9]. This deficiency is significant, as pore size can influence diffusion resistance, surface interactions, steric compatibility with drug molecules, and intracellular processing pathways. In the absence of a pore-centric perspective, it is difficult to ascertain if the enhanced biological performance observed for specific carriers is due to their chemical composition, porosity, or a relationship between the two factors.

Significant variability in drug classes, release profiles, assay conditions, and colon cancer cell models further complicates the available evidence [10]. What is lacking is a systematic, cross-platform comparison that assesses porous carriers based on pore size while incorporating cytotoxicity results across diverse experimental designs.

This study does a PRISMA-aligned systematic review, including over two thousand screened records and 203 eligible studies [11]. Our study topic is: Does pore size, classified according to the IUPAC framework, independently correlate with in vitro cytotoxic efficacy in colon cancer models? [12].

This evaluation employs a normalization-centered analytical methodology to achieve suitable comparability among investigations, given the significant variability of reported IC₅₀ values in the literature [13,14]. IC₅₀ datasets were specifically processed using Box–Cox normalization to mitigate skewness and stabilize variance across pore-size categories [15]. Subsequent to transformation, Q–Q plots were utilized to evaluate the degree of distributional normality attained and to confirm the appropriateness of the data for parametric statistical analysis [16].

A two-way ANOVA was conducted on the normalized dataset to assess the independent or interactive effects of pore-size classification, according to the IUPAC framework, and the colon cancer cell model on in vitro cytotoxic performance [17,18]. In this analysis, pore type and cell line were considered two separate explanatory variables. This methodology enables the investigation to ascertain both the primary influence of pore-size on IC₅₀ values and the systematic variation of cytotoxic responses among cell lines, in addition to identifying any statistically significant interaction between these two variables.

A two-way ANOVA is appropriate for this analysis because the dataset includes several cell models and multiple pore-size categories, both of which can influence the biological response simultaneously [19,20].

The method partitions the variation into main and interaction effects, making it possible to distinguish pore-size trends from cell line-specific differences.

As a result, any observed changes in cytotoxicity can be interpreted as genuine cross-platform patterns rather than artifacts caused by the inherent heterogeneity of colon cancer model systems.

1.1. Objective

To systematically assess the impact of pore type and porous morphology on the anticancer efficacy (IC₅₀, viability, and cytotoxicity) of porous drug-delivery devices evaluated in in vitro colon cancer models.

2. Materials and Methods

2.1. Registration

This protocol has been prospectively filed in PROSPERO with the registration number CRD420251108499, dated 20 July 2025. Any further revisions will be documented in the PROSPERO registry [21].

2.2. PICOS framework

- **Population:** In vitro models of colon cancer cells were assessed for cytotoxicity or anticancer efficacy.
- **Intervention:** Porous drug delivery systems (DDSs) featuring micro-, meso-, or macroporous structures, where the pore type was either explicitly stated or could be deduced from the morphological data presented in the article (e.g., pore size details, structural characterization, or descriptive morphological observations) [22].
- **Comparator:** The comparator could be either an unmedicated control, an inert carrier/drug delivery system, or alternative porous substances.
- **Outcomes:** Principal outcomes: IC₅₀ values and cellular viability. Secondary outcomes: Properties linked to surface characteristics, pore size and type, and additional morphology-dependent descriptors documented in the included research.
- **Study design:** The research methodology involved conducting original in vitro experimental investigations.

2.3. Eligibility Criteria

2.3.1. Inclusion Criteria

The eligibility criteria includes conducting initial in vitro investigations on colon cancer models.

The use of porous drug delivery systems, whether micro-, meso-, or macroporous, is a requirement.

The study ensures the accessibility of IC₅₀ values or extractable dose-response data.

The article contains adequate morphology-related information to categorize pore type, including pore-size statistics, structural properties, and descriptive morphological reporting.

2.3.2. Exclusion Criteria

The study excludes research that uses colon cancer models. There should be no assessment of cytotoxicity or cell viability. Impermeable systems.

The literature includes reviews, patents, books, conference abstracts, and secondary research.

Absence of extractable IC₅₀ or inadequate morphology-related data.

2.4. Search Strategy

This systematic review was performed in compliance with PRISMA 2020 principles. A comprehensive search was performed across three electronic databases Scopus, Web of Science Core Collection, and Google Scholar to ensure extensive coverage of materials science, chemistry, nanotechnology, and biomedical literature relevant to porous drug-delivery systems for colon cancer.

The search for Scopus and Web of Science was confined to papers from 2015 to 2025, corresponding to the era when modern porous structures and contemporary drug-delivery techniques gained prominence. In Google Scholar, which indexes a broader and less organized array of sources, the search parameters were confined to 2019–2025 to minimize irrelevant results from non-curated entries while maintaining adequate sensitivity for recent advancements. A three-block Boolean framework was employed, utilizing language pertinent to porous materials, anticancer drug delivery, and colorectal cancers, while omitting non-original research. The fundamental Boolean query was

("hydrogel" OR "magnetic hydrogel" OR "MOF" OR "COF" OR "ZIP" OR "porous structure*" OR "pore size" OR "mesoporous silica" OR "mesoporous carbon" OR "mesoporous" OR "macroporous" OR "nanoporous" OR "zeolite" OR "diatom" OR "HAP" OR "ceramic*" OR "MSN") AND ("drug delivery" OR "anticancer drug*") AND ("colon cancer") NOT ("review" OR "thesis" OR "book" OR "patent")

Database-specific modifications were implemented as necessary, encompassing field tags, truncation protocols, and filters for dates or document types. The comprehensive search strings for Scopus, Web of Science, and Google Scholar, along with all implemented filters, are included in the Supporting Information to guarantee perfect repeatability. The date of the last search and the deduplication process are also recorded.

The selection of studies is depicted in a PRISMA 2020 flow diagram, including the quantity of retrieved records, duplicates eliminated, titles and abstracts evaluated, full texts reviewed, reasons for exclusion, and the final collection of studies incorporated in the qualitative synthesis.

2.5. Study Selection

Two impartial evaluators assessed the titles and abstracts of all obtained records to ascertain possible eligibility. The complete texts of the chosen publications were thereafter examined independently to verify inclusion based on the established criteria. Discrepancies between the two reviewers' decisions were addressed through discussion and, as required, by consulting a third senior reviewer. The inter-reviewer agreement in the screening phase was measured using Cohen's kappa coefficient to guarantee methodological reliability.

2.6. Data Extraction

The data extraction occurred in two phases. In Stage 1, information pertaining to materials—including material classification, pore category, pore morphology, and structural descriptors—was extracted. Poor categorization was estimated by two reviewers based on structural or characterization data where pore size was not explicitly stated, with consensus achieved through debate.

IC₅₀ values were obtained in Stage 2. Numerical IC₅₀ values were recorded directly from the investigations. In instances where the IC₅₀ was not numerically specified, the dose–response curve (illustrating cell viability against concentration) was digitized utilizing WebPlotDigitizer (v4.6) to ascertain the IC₅₀ value [23]. An Excel file specifically for IC₅₀ extraction recorded the extraction methodology (direct, converted, or digitized), unit-standardization procedures, and method-specific annotations. Every submission was designated a quality flag to guarantee traceability and consistency among experiments.

2.7. Risk of Bias Assessment

The risk of bias for the included in vitro cytotoxicity studies was evaluated using a structured checklist derived from recognized quality frameworks for laboratory research, incorporating elements from QUIN, SciRAP, and NIH criteria for in-vitro methodology [24–26]. The modified assessment tool consisted of six methodological domains:

Assay validity: suitability of the cytotoxicity or viability assay, accurate readout conditions, and application of validated techniques.

Ensure transparency: provide clarity and comprehensiveness in the reporting of biological/technical replicates and sample size.

Assessment of control adequacy: characterization and suitability of negative and positive controls employed in cytotoxicity assays. Integrity of dose–response: clarity, completeness, and internal consistency of the dose–response assessment.

Outcome reporting for IC₅₀ refers to the reliability of the inhibitory concentration values that are presented.

This reliability is usually classified into three levels.

IC₅₀ values fall into the lowest concern tier when they are reported directly in common units, such as μM or μg/mL.

Reporting results in these established units is widely practiced, which contributes to their overall credibility.

IC₅₀ was reported with non-standard, incomplete, or inconsistent units necessitating unit conversion: assessed as unclear concern (1) due to conversion-related ambiguity.

IC₅₀ is not quantitatively stated and is derived from dose–response curves via WebPlotDigitizer (v4.6): categorized as high concern (0) due to variability dependent on digitization [23].

Outcome completeness: the presence of numerical data, the ability to derive curves, and the uniformity among text, figures, and supplementary resources.

Each domain was scored using a three-level scale (2 = low concern, 1 = unclear, 0 = high concern), yielding an overall quality score ranging from 0 to 12 for each study. Following laboratory-quality evaluation practices, studies were classified as:

0–4 = high risk of bias,

5–8 = unclear risk,

9–12 = low risk.

Two reviewers conducted all risk of bias evaluations independently. In studies necessitating digitization, both reviewers separately extracted IC₅₀ values from dose–response plots via WebPlotDigitizer, and disagreements were reconciled through discussion to reduce extraction-related errors [23]. Inter-reviewer agreement was assessed using Cohen’s kappa, with kappa values and domain-level scoring summaries provided in the Supporting Information.

2.8. Statistical Analysis

IC₅₀ values were descriptively summarized within each pore size category utilizing measures of central tendency and dispersion, including median, interquartile range, range, standard deviation, and coefficient of variation [27]. To mitigate skewness and stabilize variance across studies, IC₅₀ values were transformed via the Box-Cox procedure prior to inferential analysis.

Due to significant clinical and methodological heterogeneity among trials, no quantitative meta-analysis (no aggregated effect size) was conducted [15]. A two-way analysis of variance (ANOVA) was employed on Box–Cox–transformed IC₅₀ values to evaluate the primary impacts of cell line and pore-size category, together with their interaction (Cell × Pore Type) [28]. Statistical significance was established at $p < 0.05$. Polynomial curve fitting was utilized solely as a descriptive instrument and was not employed for formal hypothesis testing.

All statistical analyses (Box–Cox transformation, two-way ANOVA, post-hoc tests) and machine-learning models (Linear Regression, Random Forest, XGBoost, SVR, Gaussian Process, MLP, UMAP, t-SNE, Kernel PCA, SOM, and GMM) were implemented in Python (v3.10) [15,28–39].

3. Results

3.1 Overview of Dataset

A total of 203 studies met the inclusion criteria and were categorized using the IUPAC pore-size framework.

Within this group, 131 systems were identified as mesoporous, 38 as macroporous, 32 as microporous, and 2 as micro–mesoporous hybrids.

These studies cover a broad range of porous materials applied in colon cancer models, including including MOFs, COFs, hydrogels, zeolites, nanocellulose, micelles, and polymeric hybrids [40–46].

Each material type presents distinct structural features and corresponding drug-release behavior.

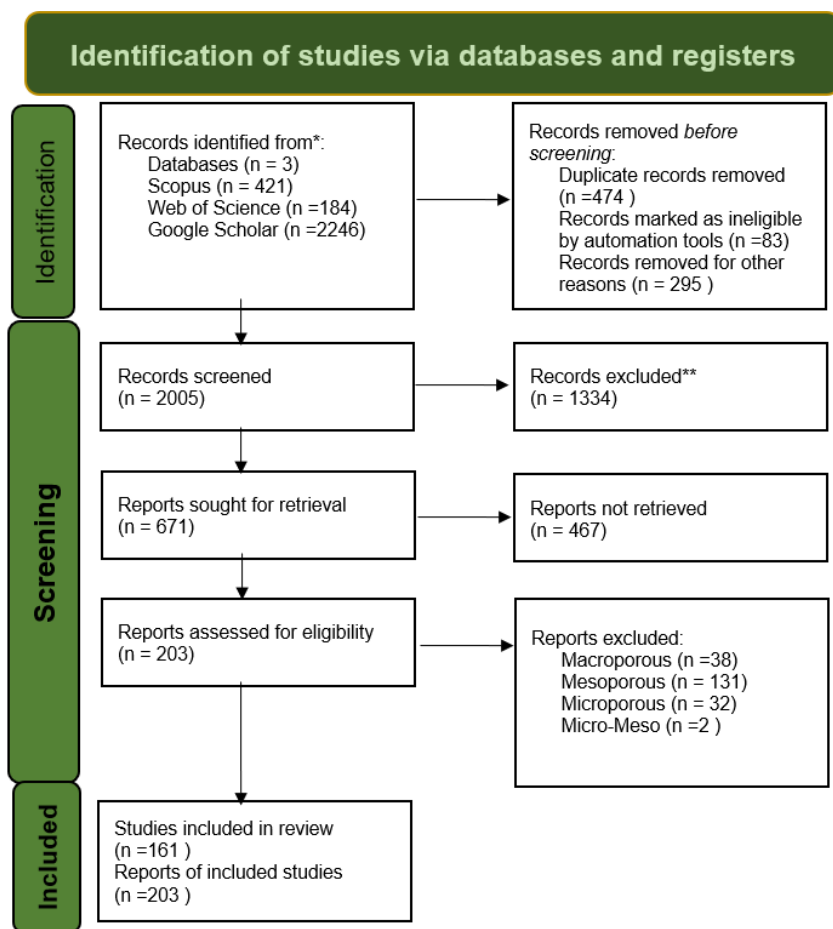


Figure 1: PRISMA Flow Diagram Illustrating the Identification of Studies Through Database and Registry Searches

3.2 Classification of Porous Systems for Colon Cancer Therapy

This section categorizes porous systems intended for colon cancer therapy according to the International Union of Pure and Applied Chemistry (IUPAC) definition of porosity, which classifies materials based on their average pore diameter as follows [9]:

Microporous systems: pores with dimensions less than 2 nanometers (nm).

Mesoporous systems: pores having sizes between 2 and 50 nanometers.

Macroporous systems: pores with sizes exceeding 50 nm.

This IUPAC-based classification provides a structured framework for analyzing the relationship between pore size, drug permeability, and therapeutic efficacy in advanced drug delivery systems. It facilitates a detailed comprehension of how structural porosity influences diffusion behavior, drug release kinetics, and overall biological efficacy. Figure 2 demonstrates that the predominant materials are mesoporous, succeeded by macroporous and microporous types. Subsequent sections will elaborate on each porosity category, emphasizing their structural characteristics, drug release mechanisms, and biological implications pertinent to colon cancer therapy [9]

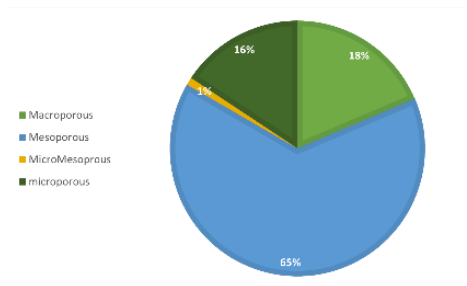


Figure 2: The Majority of Materials Fall Within the Mesoporous Regime (132 Samples, 65%), Followed by Macroporous Structures (38 Samples, 18%) And Microporous Structures (32 Samples, 16%).

3.3. Analysis of Yearly Trends and their Impact on Data Structure

The annual distribution of porous materials indicated that, recently, research efforts have predominantly focused on mesoporous systems. The excessive focus resulted in a markedly increased

variance and noise level within the mesoporous subgroup, as these studies include a wide range of material types, drug categories, loading methods, and assay conditions. As a result, the raw IC₅₀ dataset displayed significant heterogeneity, rendering direct cross-group comparisons invalid and statistically skewed.

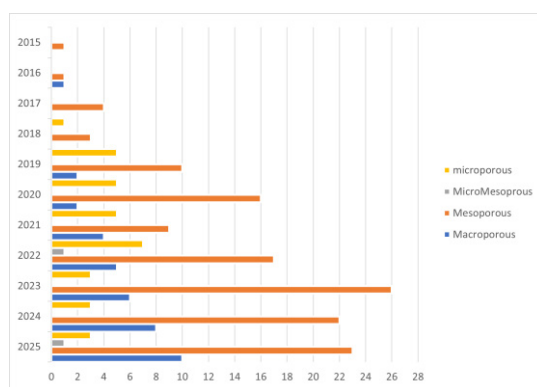


Figure 3: Yearly distribution of porous

3.4 Variability of IC₅₀ across Pore Categories

The analysis of IC₅₀ values revealed significant variation within the groups of macroporous, mesoporous, and microporous designs. Macroporous materials exhibited a moderately broad range (range = 430 μM; median ≈ 24 μM; CV ≈ 1.66). Mesoporous systems had the greatest variability (range: 0.005–9354 μM; CV

> 6), despite possessing the lowest median (~12 μM), influenced by severe outliers. Microporous structures demonstrated the most restricted range (~300 μM; CV = 1.50) while maintaining significant dispersion. The overlapping interquartile ranges across the three groups suggested an absence of a consistent or predicted correlation between pore size and cytotoxic efficacy.

	Macroporous	Mesoporous	Microporous
Range	430.17	9353.99	428.50
Medien	24.53	12.25	33.95
IQR	43.36	44.43	68.89
SD	87.34	826.91	165.75
CV	1.66	6.52	1.69
IQR-Medien	1.76	3.62	2.03

Table 1: Summarizes the Range, Median, IQR, SD, CV, and IQR-to-Median Values For Macroporous, Mesoporous, And Microporous Materials.

3.4.1. Influence of Publication Trends and Data Normalization

Recent work has indicated an overfocus on mesoporous formulations, resulting in increased variability within this subgroup due to differing chemistries, loading techniques, and

test conditions. The Box–Cox transformation enhanced normality and diminished skewness; nonetheless, the heterogeneity resulting from methodological diversity remained and obstructed significant effect-size aggregation.

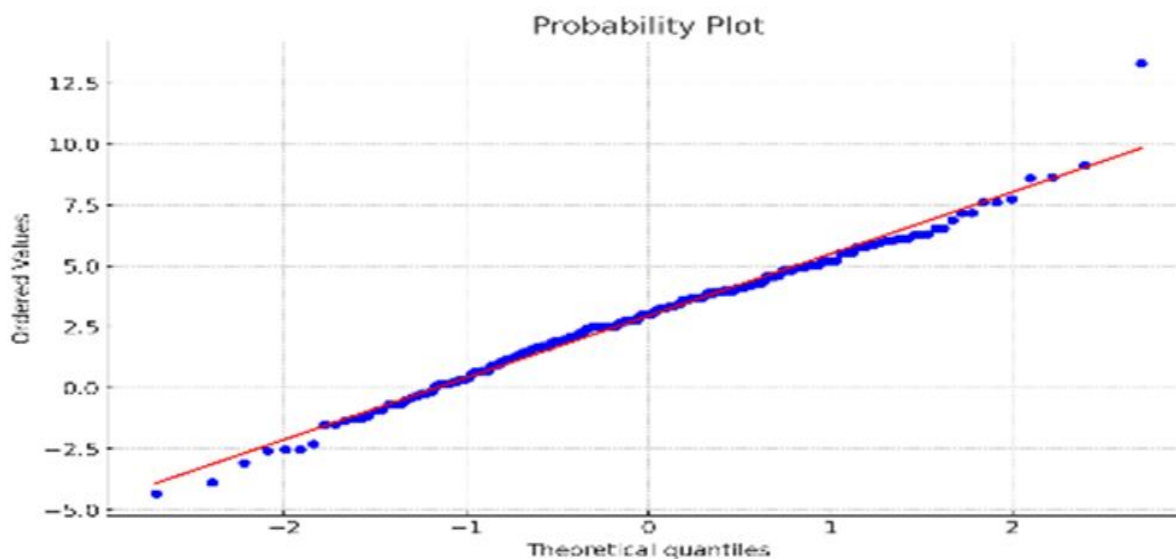


Figure 4: QQ-plot Showing Improved IC_{50} Normality After Box–Cox Transformation, While Persistent Methodological Heterogeneity Across Studies Prevents Meaningful Effect-Size Pooling.

3.4.2. Meta Analysis Feasibility

The significant diversity in experimental design, drug classes, nanoplateforms, and particularly the disproportionate sample sizes across pore categories precluded the fulfillment of assumptions necessary for meta-analysis. Thus, the research employed ANOVA-based modeling augmented by structural machine-learning methodologies.

3.5. Two-Way ANOVA

The two-way ANOVA indicated a significant main effect of cell type on IC_{50_BoxCox} values ($F = 5.96$, $p = 0.000689$). This signifies that drug sensitivity exhibits considerable variation among distinct cell lines, underscoring cell type as a crucial factor influencing IC_{50} variability. In accordance with this, significant disparities were noted in the mean IC_{50_BoxCox} values: circulating tumor cells (CTCs) and RKO displayed the lowest values (-0.22 and -0.01 , respectively), while SW480, Caco-2, and HT29 demonstrated markedly larger IC_{50} values, signifying reduced sensitivity.

The primary effect of pore type was not statistically significant ($F \approx 7.7 \times 10^{-13}$, $p = 1.0$). Despite the observation of tiny numerical differences, mesoporous materials exhibited marginally lower average IC_{50} values than microporous and macroporous structures; nonetheless, these variations lacked statistical significance. Consequently, pore architecture alone did not significantly influence overall IC_{50} variations.

Although pore type did not show a significant main effect, the analysis of the interaction between cell type and pore type revealed distinct cell-specific patterns, indicating that the optimal pore type differed across cell lines.

Macroporous structures yielded the lowest IC_{50_BoxCox} values for many cell lines (CT26, Caco-2, MC38, SW480, LS174T), whereas microporous materials proved most effective for others (HT29, RKO, SW489, LoVo, CTCs). Some cell lines, like SW620 and HeLa, responded best to mesoporous structures, while HCT116 had the lowest IC_{50} with mesoporous materials. These findings highlight a cell-dependent interaction, suggesting that the optimal pore type is not universal but changes with the cellular context.

Cell type showed a strong and statistically significant influence on the IC_{50_BoxCox} values.

In contrast, pore type did not exhibit a significant main effect.

These findings highlight the importance of considering the interaction between cell type and pore structure when evaluating material performance.

3.6. Machine Learning based Structural Analysis

A thorough examination of linear, nonlinear, supervised, and unsupervised modeling frameworks—including predictive models (linear regression, random forest, XGBoost, SVR, Gaussian process, and MLP), feature importance methodologies, and

nonlinear dimensionality-reduction techniques—revealed that the primary factor influencing drug-response variability (IC_{50}) is the biological identity of the cell line, rather than the pore type of the nanomaterial. All conventional and advanced predictive models had exceedingly inadequate performance, consistently yielding R^2 values close to zero. The multilayer perceptron accounted for merely 0.09–0.17 of the variance. The results suggest that the dataset contains a physiologically and physically intricate, low-signal structure that restricts overall prediction.

Despite the predictive models' general inability to replicate the variance structure, the permutation importance analysis in the MLP model yielded definitive insights into feature significance. The "Cell" variable had the greatest significance (0.38), whereas "Pore Type" displayed a notable yet lesser influence (0.18). This trend suggests that, even in nonlinear contexts, cell identity accounts for approximately twice the contribution of pore type to IC_{50} variability. Nonetheless, pore type is not insignificant; it serves as a minor yet discernible factor in the non-linear response landscape.

Unsupervised analysis yielded a very cohesive representation of the data's fundamental structure. UMAP demonstrated the most pronounced separation among all methodologies, elucidating distinctly defined and naturally occurring clusters that correspond to specific cell lines. Coloring the UMAP space by pore type revealed an absence of global patterns, independent clumping, and merely distributed low-intensity signals. t-SNE generated a nearly comparable structure, exhibiting distinct and persistent separation of cell lines without any clustering influenced by pore type. Kernel PCA (RBF kernel) produced a multi-cluster arrangement consistent with cell identification; however, there was no inherent categorization linked to pore type. The combined data indicate that pore type does not have significant structural influence on a wide scale and functions mainly as a contextual modulator within each cell line.

The self-organizing map (SOM) further substantiated the preeminence of cell-line architecture. Each cell line inhabited a

unique area within the two-dimensional topological grid, affirming robust spatial organization at the biological level. Pore types were extensively distributed over the map and did not aggregate in any particular area. The lack of topological consistency for pore type signifies that it does not produce a distinct structural signature; rather, it acts as a secondary modifier integrated into the overarching cell-driven architecture of IC_{50} responses.

Gaussian Mixture Modeling (GMM) validated the patterns identified in prior structure-based techniques. The optimum model comprised seven components, signifying the existence of seven latent phenotypic states within the dataset. The latent components exhibited significant overlap with the cell-line clusters found via UMAP, and none aligned with a "pure pore-type cluster." This further substantiates that the underlying architecture of IC_{50} reactions is inherently cell-driven rather than pore-driven.

Although there are no global impacts, intracellular investigations revealed that pore type has a tangible, consistent, and reproducible impact inside each cell line. Mean IC_{50} values (Box-Cox transformed) demonstrated distinctly cell-specific patterns: Macroporous nanomaterials exhibited superior performance in CT26, Caco-2, LS174T, MC38, and SW480, while microporous structures were most effective for HT29, RKO, SW489, LoVo (microporous), and CTCs. Mesoporous structures showed superiority in SW620, LoVo, Caco-2 (mesoporous), and HeLa-colon, but micro-mesoporous materials were distinctly best for HCT116. This observed variability signifies that pore-type effects are not universally weak; instead, they are markedly cell-specific and context-dependent. As a result, a universal ranking of pore types is absent among cell lines.

Graphic 5 This four-panel graphic encapsulates machine-learning evidence—feature importance, UMAP embeddings, and GMM clustering. (A) The cell line exhibits greater significance than pore type in the MLP model. (B) Distinct UMAP clustering is influenced by cell identity. (C) There is no significant clustering based on pore type. (D) Gaussian Mixture Model components correspond to cell-line structure instead of pore type.

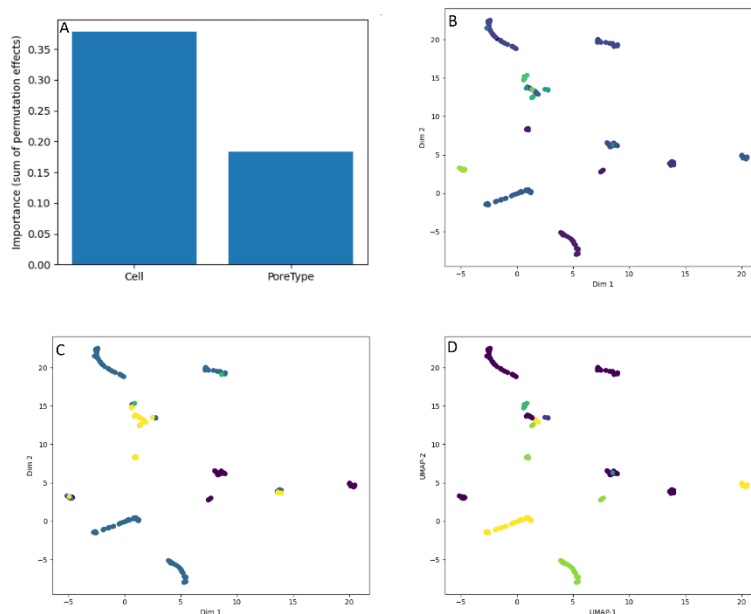


Figure 5: This four-panel figure summarizes machine-learning evidence—feature importance, UMAP embeddings, and GMM clustering (A) Greater importance of Cell Line compared to Pore Type in the MLP model. (B) Clear UMAP clustering driven by cell identity. (C) No meaningful clustering by pore type. (D) GMM components aligning with cell-line structure rather than pore type.

4. Discussion

Cancer cannot be seen merely as a chemical phenomenon; instead, its behavior arises from the complexities of metabolic pathways and physical interactions. Every cancer cell line has distinct metabolic pathways, uptake mechanisms, and intracellular trafficking characteristics, while the chemical and structural attributes of porous carriers, such as composition, pore size, and surface interactions, dictate the interaction of these systems with the cellular environment. Therefore, a significant interpretation of treatment efficacy necessitates a comprehensive chemo-biological viewpoint.

A major problem with the current literature is that it is not consistent. While researchers have thoroughly investigated specific porous structures, particularly mesoporous systems, they still lack data for many cell lines. This disparity in material coverage and biological models limits the consistent generalizability of the results.

We expect that this study provides a unified chemo-biological framework and contributes to the development of more standardized and coherent research methodologies. This study aims to identify certain porous materials and cell models that require further exploration, hence assisting future research in

the systematic development of more efficient anticancer delivery methods.

5. Conclusion

The main conclusion is that pore type is not a key factor, but cell identity is the best predictor of IC_{50} . Our findings suggest that pore type has a merely secondary impact; thus, its actual function necessitates clarification through direct investigation of its effects on cellular mechanisms and drug-release dynamics.

Authors Contributions

Sana Tat participated in data collection and manuscript drafting, and contributed to the study design as well as the analysis and interpretation of results.

Ehsan Mohebbi was involved in data collection, data analysis, and interpretation of the results.

Dr. Alireza Akbarzadeh contributed to the study conception and design and assisted in drafting the manuscript.

All authors reviewed the findings, discussed the results, and approved the final version of the manuscript for publication

Year	Composite Name	IC ₅₀ (µg.mL ⁻¹)	pore type	Category.	Ref.
2022	Bacterial nanocellulose (BNC)	10.339	Macroporous	Unclear risk	[44]
2024	MTX-MFM(Mannose-Fe ₃ O ₄ /MIL-88(Fe) (MFM))	300	Macroporous	High risk of bias	[46]
2025	CMC/HAp/ Fe ₃ O ₄	32	Macroporous	Unclear risk	[47]
2019	CS-DA/OP6 hydroge	0.24	Macroporous	Low risk	[48]
2025	Gd- CeO ₂ NPs	200	Macroporous	High risk of bias	[49]
2024	GG-SFE-ε-PL hydrogel	3.5	Macroporous	Unclear risk	[50]
2023	(BEVs) from <i>E. coli</i> strain A5922	37.94	Macroporous	Low risk	[51]
2022	FU-5/CV10	9.76	Macroporous	Low risk	[52]
2023	6MP-GPGel	36.01	Macroporous	Low risk	[53]
2025	ABZ nanosuspension	1.18	Macroporous	Low risk	[54]
2021	B-MSN (FU-5@MSN@EGCG/Fe ³⁺)	25	Macroporous	Unclear risk	[55]
2025	B(ZT)bi-metal oxides ZnO-TiO ₂	12.5	Macroporous	Unclear risk	[56]
2023	C-FA-PNP	80	Macroporous	Unclear risk	[57]
2021	CAP-MSN)CHS-GCA	117.3	Macroporous	High risk of bias	[58]
2025	chitosan-based hydrogel	2.5	Macroporous	Unclear risk	[59]
2023	CL-NBSCh micelles	11.38	Macroporous	Low risk	[60]
2024	Cur@Lac GelMA/SilMA	50	Macroporous	Unclear risk	[61]
2024	fTQ-PB	80.59	Macroporous	Low risk	[62]
2022	FA-CS-PLGA	430.25	Macroporous	High risk of bias	[63]
2016	ME/5FU	0.08	Macroporous	Low risk	[64]
2025	GN@CsNPs	30.9	Macroporous	Unclear risk	[65]
2025	GPCD hydrogels	10	Macroporous	Unclear risk	[66]
2024	FU-5-MHM	100	Macroporous	Unclear risk	[67]
2024	Hybrid lipid nanosystem (liposomes) co-loading 5-fluorouracil (FU-5) and iron oxide (Fe ₂ O ₃ /Fe ₃ O ₄)	8.1	Macroporous	Unclear risk	[68]
2019	INUAAD10 gel	50	Macroporous	Unclear risk	[69]
2025	MHBs	64	Macroporous	Unclear risk	[70]
2020	Mn _{0.5} Zn _{0.5} Fe _{2-2x} (Dy _x Y _x)O ₄ x = (0.05)	0.2	Macroporous	Unclear risk	[71]
2022	MT/SD-hydrogel	24.075	Macroporous	Unclear risk	[72]
2025	Nps Bsa Oxa	15	Macroporous	Unclear risk	[73]
2021	PNiPenPH	35.6	Macroporous	Unclear risk	[74]
2020	Ploxamer 407 (Pluronic F127)	0.5	Macroporous	Unclear risk	[75]
2025	Poly(NIPAM-co-HEMA-co-AAm) hydrogel	6.15	Macroporous	Low risk	[76]
2022	Psy-g-Poly(An-co-AA)	40	Macroporous	Unclear risk	[77]
2024	PTX(8)@BN@Gel	1.48	Macroporous	Low risk	[78]
2024	PVA-κ-Carrageenan hydrogel modified with tannic acid	125	Macroporous	High risk of bias	[79]
2021	SP-SLS-NS	20.1	Macroporous	Unclear risk	[80]
2023	Te/V-HAP@DOX-CS	0.26	Macroporous	Low risk	[81]
2023	ZnF	25	Macroporous	Unclear risk	[82]
2023	ACNF-VD-containing composite aerogel	141.2	Mesoporous	High risk of bias	[83]
2024	BA-rMSNs	0.26	Mesoporous	Low risk	[84]
2025	CaCO ₃ /CNF/SA hydrogels	16	Mesoporous	Unclear risk	[85]

2022	CS-ID@NMs + US	0.2	Mesoporous	Unclear risk	[86]
2015	NPCPT	54.75	Mesoporous	Low risk	[87]
2025	Cu/EA-MOF	60	Mesoporous	Unclear risk	[88]
2019	Cur-MSNPs	4	Mesoporous	Unclear risk	[89]
2021	DOX- Fe ₃ O ₄ @agar.	12	Mesoporous	Unclear risk	[90]
2023	doxorubicin-loaded hydrogel (50 -GMP: NAP, 16.0 mM: 4.0 mM, DOX 0.2 mM	2	Mesoporous	Unclear risk	[91]
2023	Eud-Coated TER-Loaded MSNs(SBA-15)	4.38	Mesoporous	Low risk	[92]
2021	MCFL224 nano-complexes(MOF)	1.9	Mesoporous	Unclear risk	[93]
2023	MCM*NH ₂ *HN*Cu (Cu (II)-hybrid)	70	Mesoporous	Unclear risk	[94]
2019	Oxmi-HMSN	5.68	Mesoporous	Low risk	[95]
2020	S-MTN@IG-P	30	Mesoporous	Unclear risk	[96]
2025	(DOX@MSNP-BA-Tf)	140	Mesoporous	High risk of bias	[2]
2025	(OXp/CDs/PS)@Pec hydrogel beads	50	Mesoporous	Unclear risk	[97]
2023	(Zn-MSN-NH ₂ -CP)	250	Mesoporous	High risk of bias	[98]
2021	5-FC loaded G. Mg/Clino	150	Mesoporous	High risk of bias	[99]
2025	5-Flu/MET@MSNs/Ce6@HIL	1.29	Mesoporous	Low risk	[100]
2020	FU-5 + CUR@CS/Gr/Pd	9.87	Mesoporous	Low risk	[101]
2022	FU-5 loaded Mg/Ca(NRs)	165	Mesoporous	High risk of bias	[102]
2021	FU-5-MS5)CHS-GCA	26.15	Mesoporous	Low risk	[103]
2017	FU-5@MSN-RGD	25.86	Mesoporous	Low risk	[104]
2018	FU-5@MSN-NH ₂ /GC	1.25	Mesoporous	Low risk	[105]
2022	FU-5/Cur-P@HMPB	10	Mesoporous	Unclear risk	[106]
2025	A-OHEC-APTES@1	25	Mesoporous	Unclear risk	[107]
2025	A(ZT) bi-metal oxides ZnO-TiO ₂	12	Mesoporous	Unclear risk	[56]
2021	Aft-Cu	4.92	Mesoporous	Low risk	[108]
2024	Ag/MSS/Cpt	15	Mesoporous	Unclear risk	[109]
2023	Apt-PEG-Au-NPs@FU-5	11.27	Mesoporous	Low risk	[110]
2020	Apt-PCAD-DMSN@DOX	6.25	Mesoporous	Low risk	[111]
2021	AuNPs-LY@Ge	0.056	Mesoporous	Unclear risk	[112]
2020	BGN@PDA-DOX	30	Mesoporous	Unclear risk	[113]
2019	BisBAL NPs t	5	Mesoporous	Unclear risk	[114]
2025	CH/HA PECs	18.15	Mesoporous	Low risk	[115]
2023	CaO ₂ -N770@MSN	3	Mesoporous	Unclear risk	[116]
2023	Carboplatin@N-HMSNs	30.47	Mesoporous	Low risk	[117]
2022	CatCry-AgNP-DOX	0.8	Mesoporous	Unclear risk	[118]
2019	CeO ₂ NPs	31.925	Mesoporous	Unclear risk	[119]
2022	BNC	132.402	Mesoporous	High risk of bias	[44]
2020	CFAP = COF + FeCl ₃ + Poly(p-phenylenediamine) + PEG (NH ₂ -PEG ₂₀₀₀ -COOH)	100	Mesoporous	Unclear risk	[120]
2023	Cisplatin@N-HMSNs	20.75	Mesoporous	Low risk	[117]
2023	CMC@MWCNTs@FCA	752	Mesoporous	High risk of bias	[121]
2019	CMC/LDH(Zn/Al)-FU-5	32	Mesoporous	Unclear risk	[122]
2023	CMS-Glu/SHK	0.666	Mesoporous	Unclear risk	[123]

2022	CMS@LDH(Mg–Al)@DOX,FU-5 microspheres	36	Mesoporous	Unclear risk	[124]
2020	CNT–DOX–Fe ₃ O ₄ –Tf	0.377	Mesoporous	Unclear risk	[125]
2023	CoF	30	Mesoporous	Unclear risk	[82]
2023	COF/FU-5@CMS-Gel hydrogel	70	Mesoporous	Unclear risk	[126]
2023	Col-IV@IRI-G5MNP	23.9	Mesoporous	Unclear risk	[127]
2020	Gd _{1-x} γCe _x Tb _γ BO ₃ @SiO ₂	10	Mesoporous	Unclear risk	[128]
2022	COS-DOX1	4	Mesoporous	Unclear risk	[129]
2025	CP@MSN/PB + NIR	5	Mesoporous	Unclear risk	[130]
2023	CsDAGG13/ Asp/Cur hydrogels	32	Mesoporous	Unclear risk	[131]
2025	Cu–GA/DOX@ZIF-8 (CGDZ)	2	Mesoporous	Unclear risk	[132]
2023	CuF	15	Mesoporous	Unclear risk	[82]
2020	CuS@Fe-MOF	0.4	Mesoporous	Unclear risk	[133]
2025	DMSN@Pla-Lipo	3.7	Mesoporous	Unclear risk	[134]
2023	DOX-Gel.	2	Mesoporous	Unclear risk	[91]
2021	Dox@IO-MMNs	6.93	Mesoporous	Low risk	[135]
2025	DSMC@PDA-HA	60	Mesoporous	Unclear risk	[136]
2023	Dy-NiCuZn NSF _s (0.02)	144.92	Mesoporous	High risk of bias	[137]
2017	EC-MSN-D	7	Mesoporous	Unclear risk	[138]
2023	erogel–Cur–PLP	80	Mesoporous	Unclear risk	[139]
2024	Eud-CAP-TQ-Gal-PLGANP	4.7	Mesoporous	Unclear risk	[140]
2020	FA-FE-SBA15QN	10	Mesoporous	Unclear risk	[141]
2024	Fe ₃ O ₄ -NPs	60	Mesoporous	Unclear risk	[142]
2024	GelMA-BOSU-NG	0.6	Mesoporous	Unclear risk	[143]
2024	Fe ₃ O ₄ @PDA@CaCO ₃ @CM	150	Mesoporous	High risk of bias	[144]
2021	Fe ₃ O ₄ /MSN–NH ₂	3.2	Mesoporous	Unclear risk	[145]
2024	CMD-BOSU-NG	0.5	Mesoporous	Unclear risk	[143]
2023	Fu-5 loaded b-CD/Di	200	Mesoporous	High risk of bias	[146]
2023	FU.FA@NS	0.5	Mesoporous	Unclear risk	[147]
2022	FU#(PICCS@Pd)#DOX	0.85	Mesoporous	Low risk	[148]
2022	FX@Fe ₃ O ₄ –mSiO ₂ –TA	80	Mesoporous	Unclear risk	[149]
2025	Gd _{0.825} Eu _{0.175} B ₃ O ₆ @HAP@PEG	12.5	Mesoporous	Unclear risk	[150]
2022	GDH-N/C	0.7	Mesoporous	Unclear risk	[151]
2021	DOX@GeMSNs	1.77	Mesoporous	Low risk	[152]
2024	Gi-Ag@NMOF–CS–FA	0.01	Mesoporous	Low risk	[153]
2021	DOX@GMTMSNs	1.891	Mesoporous	Unclear risk	[154]
2019	GOPEG-PCACA-FA	50.69	Mesoporous	Low risk	[155]
2024	HA-BOSU-NG	0.3	Mesoporous	Unclear risk	[143]
2025	HA@HMn/PMS	120	Mesoporous	High risk of bias	[156]
2018	HA/FMSN	1.08	Mesoporous	Low risk	[157]
2020	HAP-P-Pip9.3-GA-FA	2.4	Mesoporous	Unclear risk	[158]
2024	HAp/PANI/TD/DOX.	1.42	Mesoporous	Low risk	[159]
2024	HCPT@ZIF-90-PEG-FA	3	Mesoporous	Unclear risk	[160]
2017	HMSN	1.19	Mesoporous	Low risk	[161]
2020	HMSN-11	50	Mesoporous	Unclear risk	[6]

2020	HMSS-N=N-CS/DOX + Colon enzymes	9.41	Mesoporous	Low risk	[162]
2019	hollow CeO ₂	24.075	Mesoporous	Unclear risk	[119]
2019	hollow CeO ₂ /SiO	18.625	Mesoporous	Unclear risk	[119]
2024	Hollow Mesoporous Calcium Peroxide (HMCPN17)	400	Mesoporous	High risk of bias	[163]
2020	HPAE-PCL- b -MPEG	1000	Mesoporous	High risk of bias	[164]
2023	HSCuPPaCC	38.9	Mesoporous	Unclear risk	[165]
2025	ICT-BTO@MSNs@HA	6.25	Mesoporous	Low risk	[166]
2020	M(abc)-DOX@PDA-ICG-PEG-RGD	4	Mesoporous	Unclear risk	[167]
2025	MA@E liposomes	0.03	Mesoporous	Low risk	[168]
2018	MCM-41-PO ₃ -VOR	6.3	Mesoporous	Unclear risk	[169]
2016	MCM-48	400	Mesoporous	High risk of bias	[170]
2024	MET&3-BrPA@ZIF-90@F127 (M&B@MOF)	20.2	Mesoporous	Unclear risk	[171]
2022	MMSN-EDTA@HA-Pt	8.03	Mesoporous	Low risk	[172]
2025	MNPs/DOX	10	Mesoporous	Unclear risk	[173]
2023	MPDA-Fe(III)-DOX-HA-NIR	15	Mesoporous	Unclear risk	[174]
2022	MS@FU-5#Azo	4.6	Mesoporous	Unclear risk	[175]
2025	MSN-S-S-ALG@Cur/Q	76.62	Mesoporous	Low risk	[176]
2017	MSNPs-Rh ₂ -FITC	7.5	Mesoporous	Unclear risk	[177]
2022	MSNs-DOX	15	Mesoporous	Unclear risk	[178]
2024	MSNs-PDPA-co-PGMA	733	Mesoporous	High risk of bias	[179]
2024	MSNs@NH ₂ -CLB	27.67	Mesoporous	Low risk	[180]
2020	MSNsPCOL/CG-FA	17.4	Mesoporous	Unclear risk	[181]
2024	NH ₂ -MIL-101(Fe)@GO@Luteolin@Matrine (MGD)	70	Mesoporous	Unclear risk	[182]
2025	NiO-CMC-Dcar	10	Mesoporous	Unclear risk	[183]
2022	NMOF-CS-FA-MTX	0.005	Mesoporous	Unclear risk	[184]
2023	OX@Se-MnP	65	Mesoporous	Unclear risk	[185]
2023	Oxalipalladium@N-HMSNs	42.82	Mesoporous	Low risk	[117]
2023	Oxaliplatin@N-HMSNs	19.28	Mesoporous	Low risk	[117]
2019	P3DL/PAH/PSSCMA	25	Mesoporous	Unclear risk	[186]
2022	PBNC60@m-SiO ₂ @HA@DOX	21	Mesoporous	Unclear risk	[187]
2024	PCDP (HPB@CaO ₂ /DOX-PAA)	10	Mesoporous	Unclear risk	[188]
2025	pure hydrogel(AmPec-GAA15)	2.5	Mesoporous	Unclear risk	[189]
2022	Fe-BDC-PEG@FU-5	18	Mesoporous	Unclear risk	[190]
2024	RA	65	Mesoporous	Unclear risk	[191]
2025	SA/HAp-Fe ₃ O ₄	32	Mesoporous	Unclear risk	[192]
2019	SPASNs@DOX@AS1411	5	Mesoporous	Unclear risk	[193]
2024	SPION@MSN-EPI/pDNA-ZIF-8-PEG-Apt	12	Mesoporous	Unclear risk	[194]
2022	St@Fu-5@GQDs@Bio-MOF	6.15	Mesoporous	Low risk	[195]
2025	Sul-IRMOF-ACA-HA@Sily	9.35	Mesoporous	Low risk	[196]
2025	Syloid 244FP #F3	40	Mesoporous	Unclear risk	[197]
2024	TPZ@Cu ₂ Cl(OH) ₃ -HA (TCuH)	100	Mesoporous	Unclear risk	[198]
2024	ZnO-chitosan nanocomposite	9354	Mesoporous	High risk of bias	[199]
2025	FU-5@SiO ₂	37.78	microporous	Low risk	[200]

2019	DOX-loaded MANP-N 3 -FA	120	microporous	High risk of bias	[201]
2020	HKUST-1	12.5	microporous	Unclear risk	[202]
2021	PEG-Au-NPs@DOX	9.72	microporous	Low risk	[203]
2021	FU-5-loaded CMC/PAA/St-Fe3O4 3%	32	microporous	Unclear risk	[204]
2021	FU-5@LTL	0.06	microporous	Low risk	[205]
2022	FU-5@MOF-801	65.55	microporous	Low risk	[206]
2018	FU-5@MSN-NH2/GC+LV@MSN-COOH/GC on	7	microporous	Unclear risk	[207]
2021	FU-5@NaY	0.06	microporous	Low risk	[205]
2019	FU-5-AMSN-Alg/FA-CMCT-Gel-BDC	20	microporous	Unclear risk	[208]
2025	Apt-PEG-MOF@DOX	1.4	microporous	Unclear risk	[209]
2020	COF-B + Laser	60	microporous	Unclear risk	[210]
2020	COF@ICG@OVA(CIO + PDT)	12.5	microporous	Unclear risk	[211]
2023	CS/OD/MTX/TFPM	14	microporous	Unclear risk	[211]
2025	Dox/PAA-ZIF-8-3	2.85	microporous	Low risk	[212]
2024	GG@CsNP3/FU-5 hydrogel	6	microporous	Unclear risk	[213]
2020	magMOF@GOD	0.8	microporous	Unclear risk	[214]
2022	Magnetic UiO-66-NH ₂ (MU)(OX)	18.47	microporous	Low risk	[215]
2024	MIL-125-NH ₂	1.2	microporous	Unclear risk	[216]
2022	MSN-NH ₂ -Cur-AOS	30	microporous	Unclear risk	[217]
2022	OXA-CuS@UiO-66-NH ₂	7.97	microporous	Low risk	[218]
2024	PCN-224/Au-NPs	300	microporous	High risk of bias	[219]
2022	Pectin/curcumin@bio-MOF-11	10	microporous	Unclear risk	[220]
2023	PEI-Se-MCM41@FU-5 (PBS)	24.6	microporous	Unclear risk	[221]
2023	Res@ZIF-8/TA	5	microporous	Unclear risk	[222]
2019	Faujasite-NaX (ZX)	168.3	microporous	High risk of bias	[223]
2022	TANEB hydrogel	16.38	microporous	Low risk	[224]
2022	TMU-6(RL1)	100	microporous	Unclear risk	[225]
2019	Zeolite A (ZA)	127.6	microporous	High risk of bias	[223]
2021	ZIF-8 NPs	35	microporous	Unclear risk	[226]
2020	Zr ₆ O ₄ (OH) ₄ (TCPP) ₃ (PCN-223 MOF)	70	microporous	Unclear risk	[227]
2019	ZSM-5	170.8	microporous	High risk of bias	[223]
2022	TrzTFPPPOP	3.25	MicroMesoporous	Low risk	[228]
2025	COF@IRI	40	MicroMesoporous	Unclear risk	[229]

Table S1.

References

1. Tao, S. L., & Desai, T. A. (2003). Microfabricated drug delivery systems: from particles to pores. *Advanced drug delivery reviews*, 55(3), 315-328.
2. Lee, H. Y., Thirumalaivasan, N., & Wu, S. P. (2025). H₂O₂-responsive boronic ester-modified mesoporous silica nanocarrier for TfR mediated tumor-specific drug delivery applications. *ACS Applied Bio Materials*, 8(7), 6079-6087.
3. An, Q., Dai, Z., Zhang, J., Hu, H., Wang, J., Cao, X., ... & Zheng, X. (2024). Nanoparticle Composites Comprised of Hyaluronic Acid-Decorated Metal-Organic Frameworks with Encapsulated l-Buthionine Sulfoximine and Chlorin e6 for Chemodynamic/Photodynamic Synergistic Cancer Therapy. *ACS Applied Nano Materials*, 7(10), 11757-11766.
4. Gao, J., Li, M., Chen, H., Xu, Z., Li, J., Kong, Y., & Zuo, X. (2025). Synthesis of stimuli-responsive copolymeric hydrogels for temperature, reduction and pH-controlled drug delivery. *Journal of Industrial and Engineering Chemistry*, 143, 252-261.
5. Al-Ani, I. H. (2024). Preparation and evaluation of biological activity of ZSM-5 nanoparticles loaded with gefitinib for the treatment of non-small cell lung carcinoma. *Pharmacia/*

6. Perez-Garnes, M., Gutierrez-Salmeron, M., Morales, V., Chocarro-Calvo, A., Sanz, R., Garcia-Jimenez, C., & Garcia-Munoz, R. A. (2020). Engineering hollow mesoporous silica nanoparticles to increase cytotoxicity. *Materials Science and Engineering: C*, *112*, 110935.
7. Cauda, V., Mühlstein, L., Onida, B., & Bein, T. (2009). Tuning drug uptake and release rates through different morphologies and pore diameters of confined mesoporous silica. *Microporous and Mesoporous Materials*, *118*(1-3), 435-442.
8. Arruebo, M. (2012). Drug delivery from structured porous inorganic materials. *Wiley Interdisciplinary Reviews: Nanomedicine and Nanobiotechnology*, *4*(1), 16-30.
9. Mays, T. J. (2007). A new classification of pore sizes. In *Studies in surface science and catalysis* (Vol. 160, pp. 57-62). Elsevier.
10. Yang, L., Chu, J. S., & Fix, J. A. (2002). Colon-specific drug delivery: new approaches and in vitro/in vivo evaluation. *International journal of pharmaceutics*, *235*(1-2), 1-15.
11. Tugwell, P., & Tovey, D. (2021). PRISMA 2020. *Journal of Clinical Epidemiology*, *134*, A5-A6.
12. Kuhn, H. J., Braslavsky, S. E., & Schmidt, R. (2004). Chemical actinometry. *Pure Appl. Chem*, *76*(12), 2105-2146.
13. Beeri, C., Bernstein, P. A., & Goodman, N. (1989). A sophisticate's introduction to database normalization theory. In *Readings in artificial intelligence and databases* (pp. 468-479). Morgan Kaufmann.
14. W Caldwell, G., Yan, Z., Lang, W., & A Masucci, J. (2012). The IC50 concept revisited. *Current topics in medicinal chemistry*, *12*(11), 1282-1290.
15. Osborne, J. (2010). Improving your data transformations: Applying the Box-Cox transformation. *Practical Assessment, Research, and Evaluation*, *15*(1).
16. Marden, J. I. (2004). Positions and QQ plots. *Statistical Science*, 606-614.
17. Richter, S. J., & Payton, M. E. (2005). An improvement to the aligned rank statistic for two-factor analysis of variance. *Journal of Applied Statistical Science*, *14*(3-4), 225-235.
18. Kuntz, S., Wenzel, U., & Daniel, H. (1999). Comparative analysis of the effects of flavonoids on proliferation, cytotoxicity, and apoptosis in human colon cancer cell lines. *European journal of nutrition*, *38*(3), 133-142.
19. Slinker, B. K. (1998). The statistics of synergism. *Journal of molecular and cellular cardiology*, *30*(4), 723-731.
20. Dunpall, R., & Revaprasadu, N. (2016). An in vitro and in vivo bio-interaction responses and biosafety evaluation of novel Au-ZnTe core-shell nanoparticles. *Toxicology Research*, *5*(4), 1078-1089.
21. Tat, S., Mohebbi, E., & Akbarzadeh, A. R. (2026). Impact of Surface Properties—Including Pore Size—of Porous Structures on Anticancer Drug Delivery Efficiency in Colon Cancer: A Systematic Review.
22. Vogel, H. J., & Roth, K. (2001). Quantitative morphology and network representation of soil pore structure. *Advances in water resources*, *24*(3-4), 233-242.
23. Rohatgi, A. (2017, June). *WebPlotDigitizer*.
24. Sheth, V. H., Shah, N. P., Jain, R., Bhanushali, N., & Bhatnagar, V. (2024). Development and validation of a risk-of-bias tool for assessing in vitro studies conducted in dentistry: The QUIN. *The Journal of Prosthetic Dentistry*, *131*(6), 1038-1042.
25. Roth, N., Zilliagus, J., & Beronius, A. (2021). Development of the SciRAP approach for evaluating the reliability and relevance of in vitro toxicity data. *Frontiers in Toxicology*, *3*, 746430.
26. Gibert, R., Alberti, M., Poirier, B., Jallet, C., Tordo, N., & Morgeaux, S. (2013). A relevant in vitro ELISA test in alternative to the in vivo NIH test for human rabies vaccine batch release. *Vaccine*, *31*(50), 6022-6029.
27. Wan, X., Wang, W., Liu, J., & Tong, T. (2014). Estimating the sample mean and standard deviation from the sample size, median, range and/or interquartile range. *BMC medical research methodology*, *14*(1), 135.
28. Larson, M. G. (2008). Analysis of variance. *Circulation*, *117*(1), 115-121.
29. Carbonell, J. G., Michalski, R. S., & Mitchell, T. M. (1983). An overview of machine learning. *Machine learning*, 3-23.
30. James, G., Witten, D., Hastie, T., Tibshirani, R., & Taylor, J. (2023). Linear regression. In *An introduction to statistical learning: With applications in python* (pp. 69-134). Cham: Springer international publishing.
31. Breiman, L. (2001). Random forests. *Machine learning*, *45*(1), 5-32.
32. Chen, T., He, T., Benesty, M., Khotilovich, V., Tang, Y., Cho, H., ... & Zhou, T. (2015). Xgboost: extreme gradient boosting. *R package version 0.4-2*, *1*(4), 1-4.
33. Xu, Z., Gao, Y., & Jin, Y. (2014). Application of an optimized SVR model of machine learning. *International Journal of Multimedia and Ubiquitous Engineering*, *9*(6), 67-80.
34. MacKay, D. J. (1998). Introduction to Gaussian processes. *NATO ASI series F computer and systems sciences*, *168*, 133-166.
35. Taud, H., & Mas, J. F. (2017). Multilayer perceptron (MLP). In *Geomatic approaches for modeling land change scenarios* (pp. 451-455). Cham: Springer International Publishing.
36. McInnes, L., Healy, J., & Melville, J. (2018). Umap: Uniform manifold approximation and projection for dimension reduction. *arXiv preprint arXiv:1802.03426*.
37. Song, W., Wang, L., Liu, P., & Choo, K. K. R. (2019). Improved t-SNE based manifold dimensional reduction for remote sensing data processing. *Multimedia Tools and Applications*, *78*(4), 4311-4326.
38. Mika, S., Schölkopf, B., Smola, A., Müller, K. R., Scholz, M., & Rätsch, G. (1998). Kernel PCA and de-noising in feature spaces. *Advances in neural information processing systems*, *11*.
39. Berkowitz, D., Cohen, J. S., McCollum, N., Rojas, C. R., & Chamberlain, J. M. (2023). Delays in treatment and disposition attributable to undertriage of pediatric emergency medicine

- patients. *The American journal of emergency medicine*, 74, 130-134.
40. Soleimani Abhari, P., Habibi, B., & Morsali, A. (2024). Selective adsorption of Hg (II) ions using functionalized Zr mixed-linker MOFs. *Crystal Growth & Design*, 24(8), 3491-3500.
 41. Song, S., Wang, D., Zhao, K., Wu, Y., Zhang, P., Liu, J., ... & Liu, Z. (2022). Donor-acceptor structured photothermal COFs for enhanced starvation therapy. *Chemical Engineering Journal*, 442, 135963.
 42. Mehta, P., Mahadik, K., Kadam, S., & Dhapte-Pawar, V. (2021). Advanced applications of green hydrogels in drug delivery systems. *Applications of advanced green materials*, 89-130.
 43. Jiang, P., Hu, Y., & Li, G. (2019). Biocompatible Au@Ag nanorod@ZIF-8 core-shell nanoparticles for surface-enhanced Raman scattering imaging and drug delivery. *Talanta*, 200, 212-217.
 44. Martínez, E., Osorio, M., Finkielstein, C., Ortiz, I., Peresin, M. S., & Castro, C. (2022). 5-Fluorouracil drug delivery system based on bacterial nanocellulose for colorectal cancer treatment: Mathematical and in vitro evaluation. *International journal of biological macromolecules*, 220, 802-815.
 45. Huang, S., & Huang, G. (2020). Design and application of dextran carrier. *Journal of Drug Delivery Science and Technology*, 55, 101392.
 46. Poursadegh, H., Amini-Fazl, M. S., Javanbakht, S., & Kazeminava, F. (2024). Magnetic nanocomposite through coating mannose-functionalized metal-organic framework with biopolymeric pectin hydrogel beads: a potential targeted anticancer oral delivery system. *International Journal of Biological Macromolecules*, 254, 127702.
 47. Foroutan, R., Mohammadzadeh, A., Mohammadi, R., & Javanbakht, S. (2025). Carboxymethyl cellulose/hydroxyapatite/Fe₃O₄ bio-nanocomposite hydrogel beads: an efficient oral pH-responsive carrier for doxorubicin delivery. *Chemical Papers*, 79(4), 2461-2470.
 48. Liang, Y., Zhao, X., Ma, P. X., Guo, B., Du, Y., & Han, X. (2019). pH-responsive injectable hydrogels with mucosal adhesiveness based on chitosan-grafted-dihydrocaffeic acid and oxidized pullulan for localized drug delivery. *Journal of colloid and interface science*, 536, 224-234.
 49. Sarangi, S., Suryakanta, U., Nayak, N., Mandal, D., & Sahoo, T. R. (2025). Green synthesis and characterization of Gd-doped CeO₂ NPs and their anticancer effects against colon cancer and breast cancer. *Journal of Rare Earths*.
 50. Qu, Y., Li, X., Chen, X., Li, J., Yu, Z., & Shen, R. (2024). Novel pH-sensitive gellan gum-ε-polylysine hydrogel microspheres for sulforaphane delivery. *Journal of the Science of Food and Agriculture*, 104(15), 9423-9433.
 51. Marzoog, T. R., Jabir, M. S., Ibraheem, S., Jawad, S. F., Hamzah, S. S., Sulaiman, G. M., ... & Khan, R. A. (2023). Bacterial extracellular vesicles induced oxidative stress and mitophagy through mTOR pathways in colon cancer cells, HT-29: Implications for bioactivity. *Biochimica et Biophysica Acta (BBA)-Molecular Cell Research*, 1870(6), 119486.
 52. Salahuddin, N., Awad, S., & Elfiky, M. (2022). Vanillin-crosslinked chitosan/ZnO nanocomposites as a drug delivery system for 5-fluorouracil: study on the release behavior via mesoporous ZrO₂-Co₃O₄ nanoparticles modified sensor and antitumor activity. *RSC advances*, 12(33), 21422-21439.
 53. Kim, S., Lee, W., Park, H., & Kim, K. (2023). Tumor microenvironment-responsive 6-mercaptopurine-releasing injectable hydrogel for colon cancer treatment. *Gels*, 9(4), 319.
 54. Guo, Y., Patel, H. J., Patel, A. S., Squillante, E., & Patel, K. (2025). Albendazole nanosuspension coated granules for the rapid localized release and treatment of colorectal cancer. *Colloids and Surfaces B: Biointerfaces*, 245, 114320.
 55. Chen, Z. X., Li, J. L., Pan, P., Bao, P., Zeng, X., & Zhang, X. Z. (2021). Combination gut microbiota modulation and chemotherapy for orthotopic colorectal cancer therapy. *Nano Today*, 41, 101329.
 56. Khalaf, M. M., Shaaban, S., Abd El-Lateef, H. M., Althikrallah, H. A., Mohamed, I. M., Sharaky, M., ... & Al-Karmalawy, A. A. (2025). Innovative TiO₂/ZnO-organoselenium composites with diselenide linkages for enhanced anticancer efficacy. *New Journal of Chemistry*, 49(12), 4887-4900.
 57. Bhaskaran, N. A., Jitta, S. R., Kumar, L., Sharma, P., Kulkarni, O. P., Hari, G., ... & Bhaskar, K. V. (2023). Folic acid-chitosan functionalized polymeric nanocarriers to treat colon cancer. *International Journal of Biological Macromolecules*, 253, 127142.
 58. Narayan, R., Gadag, S., Cheruku, S. P., Raichur, A. M., Day, C. M., Garg, S., ... & Nayak, U. Y. (2021). Chitosan-glucuronic acid conjugate coated mesoporous silica nanoparticles: A smart pH-responsive and receptor-targeted system for colorectal cancer therapy. *Carbohydrate polymers*, 261, 117893.
 59. Wang, L., Mei, Z., Jin, G., Liu, H., Lv, S., Fu, R., ... & Yao, C. (2024). In situ sustained release hydrogel system delivering GLUT1 inhibitor and chemo-drug for cancer post-surgical treatment. *Bioactive Materials*, 36, 541-550.
 60. Sripethong, S., Eze, F. N., Sajomsang, W., & Ovatlarnporn, C. (2023). Development of pH-Responsive N-benzyl-N-O-succinyl Chitosan Micelles Loaded with a Curcumin Analog (Cyqualone) for Treatment of Colon Cancer. *Molecules*, 28(6), 2693.
 61. Zhang, B., Yan, J., Jin, Y., Yang, Y., & Zhao, X. (2024). Curcumin-shellac nanoparticle-loaded GelMA/SilMA hydrogel for colorectal cancer therapy. *European Journal of Pharmaceutics and Biopharmaceutics*, 202, 114409.
 62. Alfatama, M., Choukaife, H., Al Rahal, O., & Zin, N. Z. M. (2024). Thymoquinone pectin beads produced via electrospray: enhancing oral targeted delivery for colorectal cancer therapy. *Pharmaceutics*, 16(11), 1460.
 63. Rahmati, A., Homayouni Tabrizi, M., Karimi, E., & Zarei, B. (2022). Fabrication and assessment of folic acid conjugated-chitosan modified PLGA nanoparticle for delivery of alpha terpineol in colon cancer. *Journal of Biomaterials Science, Polymer Edition*, 33(10), 1289-1307.

64. Sadeghi-Abandansari, H., Pakian, S., Nabid, M. R., Ebrahimi, M., & Rezalotfi, A. (2021). Local co-delivery of 5-fluorouracil and curcumin using Schiff's base cross-linked injectable hydrogels for colorectal cancer combination therapy. *European Polymer Journal*, *157*, 110646.
65. Abdelaziz, M. A., Alalawy, A. I., Sobhi, M., Alatawi, O. M., & Alaysuy, O. (2025). Development and characterization of engineered gingerol loaded chitosan nanoparticles for targeting colon cancer, bacterial infection, and oxidative stress mitigation. *International Journal of Biological Macromolecules*, 146093.
66. Jia, X., Wei, Y., Zhang, X., Gu, Q., Liu, Y., Wang, S., & Zhu, C. (2025). Dual-Drug Loaded γ -Polyglutamic Acid Hydrogel with Hydrophilic Doxorubicin and Hydrophobic Camptothecin for Enhanced Tumor Therapy. *Chemistry—An Asian Journal*, *20*(18), e00058.
67. Poursadegh, H., Bakhshi, V., Amini-Fazl, M. S., Adibag, Z., Kazeminava, F., & Javanbakht, S. (2024). Incorporating mannose-functionalized hydroxyapatite/metal-organic framework into the hyaluronic acid hydrogel film: A potential dual-targeted oral anticancer delivery system. *International Journal of Biological Macromolecules*, *274*, 133516.
68. Azevedo, A., Coelho, M. P., Pinho, J. O., Soares, P. I., Reis, C. P., Borges, J. P., & Gaspar, M. M. (2024). An alternative hybrid lipid nanosystem combining cytotoxic and magnetic properties as a tool to potentiate antitumor effect of 5-fluorouracil. *Life Sciences*, *344*, 122558.
69. Afinjuomo, F., Fouladian, P., Parikh, A., Barclay, T. G., Song, Y., & Garg, S. (2019). Preparation and characterization of oxidized inulin hydrogel for controlled drug delivery. *Pharmaceutics*, *11*(7), 356.
70. Tahmasebi, S., Farmanbordar, H., & Mohammadi, R. (2025). Synthesis of magnetic bio-nanocomposite hydrogel beads based on sodium alginate and β -cyclodextrin: Potential pH-responsive oral delivery anticancer systems for colorectal cancer. *International Journal of Biological Macromolecules*, *305*, 140748.
71. Almessiere, M. A., Slimani, Y., Rehman, S., Khan, F. A., Polat, E. G., Sadaqat, A., ... & Baykal, A. (2020). Synthesis of Dy-Y co-substituted manganese zinc spinel nanoferrites induced anti-bacterial and anti-cancer activities: Comparison between sonochemical and sol-gel auto-combustion methods. *Materials Science and Engineering: C*, *116*, 111186.
72. Wang, C. Y., Sun, M., Fan, Z., & Du, J. Z. (2022). Intestine enzyme-responsive polysaccharide-based hydrogel to open epithelial tight junctions for oral delivery of imatinib against colon cancer. *Chinese Journal of Polymer Science*, *40*(10), 1154-1164.
73. Wilson, B., Geetha, K. M., Divekar, K., Jenita, J. L., Premakumari, K. B., & Sagar, G. (2025). Albumin nanoparticle enhances oxaliplatin concentration in the colorectal region to treat colon cancer with increased efficacy. *BioNanoScience*, *15*(1), 46.
74. Carreño, G., Pereira, A., Avila-Salas, F., Marican, A., Andrade, F., Roca-Melendres, M. M., ... & Duran-Lara, E. F. (2021). Development of “on-demand” thermo-responsive hydrogels for anti-cancer drugs sustained release: Rational design, in silico prediction and in vitro validation in colon cancer models. *Materials Science and Engineering: C*, *131*, 112483.
75. Chung, C. K., García-Couce, J., Campos, Y., Kralisch, D., Bierau, K., Chan, A., ... & Cruz, L. J. (2020). Doxorubicin loaded poloxamer thermosensitive hydrogels: chemical, pharmacological and biological evaluation. *Molecules*, *25*(9), 2219.
76. Ghasemi, S., Najafi, M., Doroudian, M., Rastegari, B., Behzad-Behbahani, A., Soltanimehr, H., & Farjadian, F. (2025). Temperature-and pH-responsive poly (NIPAM-co-HEMA-co-AAm) nanogel as a smart vehicle for doxorubicin delivery; combating colorectal cancer. *Gels*, *11*(4), 227.
77. Kumar, D., Gautam, A., & Kundu, P. P. (2022). Synthesis of pH-sensitive grafted psyllium: Encapsulation of quercetin for colon cancer treatment. *Journal of Applied Polymer Science*, *139*(4), 51552.
78. Wang, T., Ding, J., Chen, Z., Zhang, Z., Rong, Y., Li, G., ... & Chen, X. (2024). Injectable, adhesive albumin nanoparticle-incorporated hydrogel for sustained localized drug delivery and efficient tumor treatment. *ACS applied materials & interfaces*, *16*(8), 9868-9879.
79. Marlina, A., Misran, M., Ndruru, S. T. C. L., Saad, H. M., & Sim, K. S. (2024). Development and Characterization of Tannic Acid-Modified PVA- κ Carrageenan Gel for Sustained Release of Lidocaine. *ChemistrySelect*, *9*(37), e202400387.
80. Taymouri, S., Ahmadi, Z., Mirian, M., & Tavakoli, N. (2021). Simvastatin nanosuspensions prepared using a combination of pH-sensitive and timed-release approaches for potential treatment of colorectal cancer. *Pharmaceutical Development and Technology*, *26*(3), 335-348.
81. Abdel Hady, M., & Ahmed, M. K. (2023). Tellurium/ Vanadate Doped Hydroxyapatite Nano-Scaffold Carrier for Doxorubicin Colon Cancer Targeting. *Egyptian Journal of Chemistry*, *66*(10), 521-528.
82. Mohana, S., & Sumathi, S. (2024). Agaricus bisporus mediated synthesis of cobalt ferrite, copper ferrite and zinc ferrite nanoparticles for hyperthermia treatment and drug delivery. *Journal of Cluster Science*, *35*(1), 129-142.
83. Bingol Ozakpinar, O., Dastan, H., Gurboga, M., Sayin, F. S., Ozsavci, D., & Caliskan Salihi, E. (2023). Carbon nanofiber—sodium alginate composite aerogels loaded with vitamin D: the cytotoxic and apoptotic effects on colon cancer cells. *Gels*, *9*(7), 561.
84. Fan, Y., Zhang, W., Iqbal, Z., Li, X., Lin, Z., Wu, Z., ... & Liu, P. (2024). Rod-shaped mesoporous silica nanoparticles reduce bufalin cardiotoxicity and inhibit colon cancer by blocking lipophagy. *Lipids in Health and Disease*, *23*(1), 318.
85. Bai, W., Chen, H., Li, J., Cai, W., Kong, Y., & Zuo, X. (2025). Calcium carbonate hollow microspheres encapsulated cellulose nanofiber/sodium alginate hydrogels as a sequential delivery system. *International journal of biological macromolecules*, *309*, 142839.
86. Cao, Y., Liu, S., Ma, Y., Ma, L., Zu, M., Sun, J., ... & Xiao,

- B. (2022). Oral nanomotor-enabled mucus traverse and tumor penetration for targeted chemo-sono-immunotherapy against colon cancer. *Small*, 18(42), 2203466.
87. Théron, C., Gallud, A., Giret, S., Maynadier, M., Grégoire, D., Puche, P., ... & Gary-Boho, M. (2015). pH-operated hybrid silica nanoparticles with multiple H-bond stoppers for colon cancer therapy. *RSC advances*, 5(80), 64932-64936.
88. Zhang, W., Zhao, M., Wang, L., Wang, J., Ge, X., Liu, J., ... & Lu, J. (2025). Dual NIR-II fluorescence and ratiometric photoacoustic imaging-guided metal-phenolic nanosheets for H₂S-activatable synergistic therapy. *iScience*, 28(5).
89. Elbially, N. S., Abd Elfatah, E., & Khalil, W. A. (2019). Cytotoxicity assessment of mesoporous silica nanoparticles-curcumin against breast and colon cancer cell lines: in vitro study. *Egyptian Journal of Chemistry*, 62(The First International Conference on Molecular Modeling and Spectroscopy 19-22 February, 2019), 125-135.
90. Wang, Y. J., Lin, P. Y., Hsieh, S. L., Kirankumar, R., Lin, H. Y., Li, J. H., ... & Hsieh, S. (2021). Utilizing edible agar as a carrier for dual functional doxorubicin-Fe₃O₄ nanotherapy drugs. *Materials*, 14(8), 1824.
91. Sarkar, S., Bera, S., Moitra, P., & Bhattacharya, S. (2023). A self-healable and injectable hydrogel for pH-responsive doxorubicin drug delivery in vitro and in vivo for colon cancer treatment. *Materials Today Chemistry*, 30, 101554.
92. Alyami, M. H., Musallam, A. A., Ibrahim, T. M., Mahdy, M. A., Elnahas, H. M., & Aldeeb, R. A. (2023). The exploitation of pH-responsive Eudragit-coated mesoporous silica nanostructures in the repurposing of terbinafine hydrochloride for targeted colon cancer inhibition: design optimization, in vitro characterization, and cytotoxicity assessment. *Pharmaceutics*, 15(12), 2677.
93. Mokri, N., Sepehri, Z., Faninam, F., Khaleghi, S., Kazemi, N. M., & Hashemi, M. (2022). Chitosan-coated Zn-metal-organic framework nanocomposites for effective targeted delivery of LNA-antisense miR-224 to colon tumor: in vitro studies. *Gene Therapy*, 29(12), 680-690.
94. Naz, A., Kumari, R., Arun, S., Narvi, S. S., Alam, M. S., & Dutta, P. K. (2023). Cu (II)-coordinated silica based mesoporous inorganic-organic hybrid material: synthesis, characterization and evaluation for drug delivery, antibacterial, antioxidant and anticancer activities. *Journal of Polymer Research*, 30(2), 76.
95. Yang, H., Liu, Y., Qiu, Y., Ding, M., & Zhang, Y. (2019). MiRNA-204-5p and oxaliplatin-loaded silica nanoparticles for enhanced tumor suppression effect in CD44-overexpressed colon adenocarcinoma. *International journal of pharmaceutics*, 566, 585-593.
96. Gautam, M., Gupta, B., Soe, Z. C., Poudel, K., Maharjan, S., Jeong, J. H., ... & Kim, J. O. (2020). Stealth Polymer-Coated Graphene Oxide Decorated Mesoporous Titania Nanoplatforams for In Vivo Chemo-Photodynamic Cancer Therapy: Gautam et al. *Pharmaceutical Research*, 37(8), 162.
97. Pooresmaeil, M., & Namazi, H. (2025). Photoluminescent oxaliplatin loaded porous starch coated with pectin biopolymer: Design, fabrication, and controlled drug delivery. *Industrial Crops and Products*, 223, 120124.
98. Sinafar, H., Noorbazargan, H., Tafvizi, F., & Naseh, V. (2023). Evaluation of apoptotic and anti-metastatic effects by modified mesoporous silica nanoparticles (MSNs) with Zn and NH₂ containing cisplatin on HT-29 cell line. *Journal of Nanoparticle Research*, 25(5), 89.
99. Othman, S. I., Allam, A. A., Al Fassam, H., Abu-Taweel, G. M., Altoom, N., & Abukhadra, M. R. (2021). Sonoco green decoration of clinoptilolite with MgO nanoparticles as a potential carrier for 5-fluorouracil drug: loading behavior, release profile, and cytotoxicity. *Journal of Inorganic and Organometallic Polymers and Materials*, 31(12), 4608-4622.
100. Wang, N., Hu, J., Jin, L., Wang, S., Zeng, B., Liu, Y., ... & Jin, M. (2025). Inulin and hyaluronic acid-based oral liposome for enhanced photo-chemotherapy against orthotopic colon cancer and its reversal effects on tumor hypoxia and intestinal microbiota. *International Journal of Biological Macromolecules*, 304, 140996.
101. Dhanavel, S., Praveena, P., Narayanan, V., & Stephen, A. (2020). Chitosan/reduced graphene oxide/Pd nanocomposites for co-delivery of 5-fluorouracil and curcumin towards HT-29 colon cancer cells. *Polymer Bulletin*, 77(11), 5681-5696.
102. Othman, S. I., Adlii, A., Allam, A. A., Alqhtani, H. A., AlHammadi, A. A., & Abukhadra, M. R. (2022). Characterization of MgO/CaO hybrid nanorods as an enhanced inorganic carrier of 5-Fluorouracil drug; loading, release, and cytotoxicity studies. *Journal of Inorganic and Organometallic Polymers and Materials*, 32(6), 2322-2331.
103. Narayan, R., Gadag, S., Mudakavi, R. J., Garg, S., Raichur, A. M., Nayak, Y., ... & Nayak, U. Y. (2021). Mesoporous silica nanoparticles capped with chitosan-glucuronic acid conjugate for pH-responsive targeted delivery of 5-fluorouracil. *Journal of Drug Delivery Science and Technology*, 63, 102472.
104. Pan, G., Jia, T. T., Huang, Q. X., Qiu, Y. Y., Xu, J., Yin, P. H., & Liu, T. (2017). Mesoporous silica nanoparticles (MSNs)-based organic/inorganic hybrid nanocarriers loading 5-Fluorouracil for the treatment of colon cancer with improved anticancer efficacy. *Colloids and Surfaces B: Biointerfaces*, 159, 375-385.
105. Liu, W., Zhu, Y., Wang, F., Li, X., Liu, X., Pang, J., & Pan, W. (2018). Galactosylated chitosan-functionalized mesoporous silica nanoparticles for efficient colon cancer cell-targeted drug delivery. *Royal Society open science*, 5(12).
106. Chen, J., Xue, F., Du, W., Yu, H., Yang, Z., Du, Q., & Chen, H. (2022). An endogenous H₂S-activated nanoplatforam for triple synergistic therapy of colorectal cancer. *Nano Letters*, 22(15), 6156-6165.
107. Cheng, Q., Fu, H., & Mao, Y. (2025). Construction of a Controlled Drug Delivery and Optical Monitoring System for Colorectal Cancer via Natural Fiber Modification. *Journal of Medical and Biological Engineering*, 45(2), 264-272.
108. Xiong, K., Zhou, Y., Karges, J., Du, K., Shen, J., Lin, M., ... & Chao, H. (2021). Autophagy-dependent apoptosis induced by apoferritin-Cu (II) nanoparticles in multidrug-resistant colon

- cancer cells. *ACS applied materials & interfaces*, 13(33), 38959-38968.
109. Rehman, S., Ravinayagam, V., Al-Jameel, S. S., Ali, S. M., Alzayer, S. Z., Alfaraj, Z. M., ... & Jermy, B. R. (2024). Controlling cisplatin release by synergistic action of silver-cisplatin on monodispersed spherical silica for targeted anticancer and antibacterial activities. *Arabian Journal of Chemistry*, 17(4), 105661.
110. Kamil Mohammad Al-Mosawi, A., Bahrami, A. R., Nekooei, S., Saljooghi, A. S., & Matin, M. M. (2023). Using magnetic mesoporous silica nanoparticles armed with EpCAM aptamer as an efficient platform for specific delivery of 5-fluorouracil to colorectal cancer cells. *Frontiers in Bioengineering and Biotechnology*, 10, 1095837.
111. Zahiri, M., Babaei, M., Abnous, K., Taghdisi, S. M., Ramezani, M., & Alibolandi, M. (2020). Hybrid nanoreservoirs based on dextran-capped dendritic mesoporous silica nanoparticles for CD133-targeted drug delivery. *Journal of Cellular Physiology*, 235(2), 1036-1050.
112. Managò, S., Tramontano, C., Delle Cave, D., Chianese, G., Zito, G., De Stefano, L., ... & Rea, I. (2021). SERS quantification of galunisertib delivery in colorectal cancer cells by plasmonic-assisted diatomite nanoparticles. *Small*, 17(34), 2101711.
113. Xue, Y., Niu, W., Wang, M., Chen, M., Guo, Y., & Lei, B. (2019). Engineering a biodegradable multifunctional antibacterial bioactive nanosystem for enhancing tumor photothermo-chemotherapy and bone regeneration. *ACS nano*, 14(1), 442-453.
114. Cabral-Romero, C., Solís-Soto, J. M., Sánchez-Pérez, Y., Pineda-Aguilar, N., Meester, I., Pérez-Carrillo, E., ... & García-Cuéllar, C. M. (2020). Antitumor activity of a hydrogel loaded with lipophilic bismuth nanoparticles on cervical, prostate, and colon human cancer cells. *Anti-cancer drugs*, 31(3), 251-259.
115. Elsayyad, N. M. E., Ibrahim, M. S., & Noshi, S. H. (2025). Sustainable pH-responsive casein/hyaluronic acid layered nanoparticles for targeted delivery of metformin to colorectal cancer. *Journal of Drug Delivery Science and Technology*, 107, 106710.
116. Wu, J., Yi, S., Cao, Y., Zu, M., Li, B., Yang, W., ... & Xiao, B. (2023). Dual-driven nanomotors enable tumor penetration and hypoxia alleviation for calcium overload-photo-immunotherapy against colorectal cancer. *Biomaterials*, 302, 122332.
117. Moghadam, M. E., Sadeghi, M., Mansouri-Torshizi, H., & Saidifar, M. (2023). High cancer selectivity and improving drug release from mesoporous silica nanoparticles in the presence of human serum albumin in cisplatin, carboplatin, oxaliplatin, and oxalipalladium treatment. *European Journal of Pharmaceutical Sciences*, 187, 106477.
118. Zhou, R., Ohulchanskyy, T. Y., Xu, Y., Ziniuk, R., Xu, H., Liu, L., & Qu, J. (2022). Tumor-microenvironment-activated NIR-II nanotheranostic platform for precise diagnosis and treatment of colon cancer. *ACS applied materials & interfaces*, 14(20), 23206-23218.
119. Rasouli, Z., Yousefi, M., Torbati, M. B., Samadi, S., & Kalateh, K. (2020). Synthesis and characterization of nanoceria-based composites and in vitro evaluation of their cytotoxicity against colon cancer. *Polyhedron*, 176, 114297.
120. Liu, S., Zhou, Y., Hu, C., Cai, L., & Pang, M. (2020). Covalent organic framework-based nanocomposite for synergetic photo-, chemodynamic-, and immunotherapies. *ACS applied materials & interfaces*, 12(39), 43456-43465.
121. Alizadeh, M. H., Pooresmaeil, M., & Namazi, H. (2023). Carboxymethyl cellulose@ multi wall carbon nanotubes functionalized with Ugi reaction as a new curcumin carrier. *International Journal of Biological Macromolecules*, 234, 123778.
122. Pooresmaeil, M., Nia, S. B., & Namazi, H. (2019). Green encapsulation of LDH (Zn/Al)-5-Fu with carboxymethyl cellulose biopolymer; new nanovehicle for oral colorectal cancer treatment. *International journal of biological macromolecules*, 139, 994-1001.
123. Wang, X., Guo, W., Han, J., Li, J., Zhao, Q., Mao, Y., & Wang, S. (2023). Oral spatial-to-point cascade targeting "sugar-coated bullets" for precise and safe chemotherapy by intervention Warburg effect. *Colloids and Surfaces B: Biointerfaces*, 222, 113108.
124. Ranjbar, E., Namazi, H., & Pooresmaeil, M. (2022). Carboxymethyl starch encapsulated 5-FU and DOX co-loaded layered double hydroxide for evaluation of its in vitro performance as a drug delivery agent. *International journal of biological macromolecules*, 201, 193-202.
125. Andhari, S. S., Wavhale, R. D., Dhobale, K. D., Tawade, B. V., Chate, G. P., Patil, Y. N., ... & Banerjee, S. S. (2020). Self-propelling targeted magneto-nanobots for deep tumor penetration and pH-responsive intracellular drug delivery. *Scientific reports*, 10(1), 4703.
126. Pooresmaeil, M., & Namazi, H. (2023). pH-sensitive carboxymethyl starch-gelatin coated COF/5-Fu for colon cancer therapy. *Industrial Crops and Products*, 202, 117102.
127. Chauhan, S., Solanki, R., Jangid, A. K., Jain, P., Pranjali, P., Patel, S., ... & Kulhari, H. (2023). Manganese nanocarrier for matrix metalloproteinase 9 responsive delivery of irinotecan for colon cancer treatment. *Journal of Industrial and Engineering Chemistry*, 128, 258-267.
128. Akman, P., Ulasan, S., Banerjee, S., & Yilmaz, A. (2020). Core/shell type, Ce³⁺ and Tb³⁺ doped GdBO₃ system: Synthesis and Celecoxib drug delivery application. *Microporous and Mesoporous Materials*, 308, 110528.
129. Yi, G., Ling, J., Jiang, Y., Lu, Y., Yang, L. Y., & Ouyang, X. K. (2022). Fabrication, characterization, and in vitro evaluation of doxorubicin-coupled chitosan oligosaccharide nanoparticles. *Journal of Molecular Structure*, 1268, 133688.
130. Wang, Z. H., Zeng, X., Huang, W., Yang, Y., Zhang, S., Yang, M., ... & Shi, J. (2025). Bioactive nanomotor enabling efficient intestinal barrier penetration for colorectal cancer therapy. *Nature Communications*, 16(1), 1678.
131. Dalei, G., Das, S., Jena, S. R., Jena, D., Nayak, J., & Samanta,

- L. (2023). In situ crosslinked dialdehyde guar gum-chitosan Schiff-base hydrogels for dual drug release in colorectal cancer therapy. *Chemical Engineering Science*, 269, 118482.
132. Vu, G. T. Q., Nguyen, L. M., Nguyen Do, K. N., Tran, D. L., Vo, T. V., Nguyen, D. H., & Vong, L. B. (2025). Preparation of metal-polyphenol modified zeolitic imidazolate framework-8 nanoparticles for cancer drug delivery. *ACS Applied Bio Materials*, 8(3), 2052-2064.
133. Wang, Z., Yu, W., Yu, N., Li, X., Feng, Y., Geng, P., ... & Chen, Z. (2020). Construction of CuS@ Fe-MOF nanoplatfoms for MRI-guided synergistic photothermal-chemo therapy of tumors. *Chemical Engineering Journal*, 400, 125877.
134. Yuan, Y., Lin, Q., Feng, H. Y., Zhang, Y., Lai, X., Zhu, M. H., ... & Fang, C. (2025). A multistage drug delivery approach for colorectal primary tumors and lymph node metastases. *Nature Communications*, 16(1), 1439.
135. El-Boubbou, K., Ali, R., Al-Humaid, S., Alhallaj, A., Lemine, O. M., Boudjelal, M., & Alkushi, A. (2021). Iron oxide mesoporous magnetic nanostructures with high surface area for enhanced and selective drug delivery to metastatic cancer cells. *Pharmaceutics*, 13(4), 553.
136. Yin, G., Zhao, H., & Lan, M. (2025). A nano drug delivery system loading drugs and chlorin e6 separately to achieve photodynamic-chemo combination therapy. *Nanomedicine*, 20(6), 559-570.
137. Korkmaz, A. D. (2023). Effect of sonochemically synthesized NiO. 4CuO. 2ZnO. 4DyxFe2-xO4 nanospinel ferrites on human colorectal carcinoma and human embryonic kidney cells. *Materials Science and Engineering: B*, 295, 116598.
138. Gao, Y., Xie, X., Li, F., Lu, Y., Li, T., Lian, S., ... & Jia, L. (2017). A novel nanomissile targeting two biomarkers and accurately bombing CTCs with doxorubicin. *Nanoscale*, 9(17), 5624-5640.
139. Izadi, Z., Rashidi, M., Derakhshankhah, H., Dolati, M., Kermanshahi, M. G., Adibi, H., & Samadian, H. (2023). Curcumin-loaded porous particles functionalized with pH-responsive cell-penetrating peptide for colorectal cancer targeted drug delivery. *RSC advances*, 13(49), 34587-34597.
140. Raikar, P. R., Dandagi, P. M., & Kumbar, V. M. (2024). An innovative synergistic combination using eudragit-coated galactosylated PLGA-pluronic nanoparticles for addressing colorectal cancer. *Journal of Drug Delivery Science and Technology*, 94, 105481.
141. Mishra, S., Manna, K., Kayal, U., Saha, M., Chatterjee, S., Chandra, D., ... & Saha, K. D. (2020). Folic acid-conjugated magnetic mesoporous silica nanoparticles loaded with quercetin: A theranostic approach for cancer management. *RSC advances*, 10(39), 23148-23164.
142. Patil, A. P., Kamble, P. A., Pandey-Tiwari, A., Shembade, U. V., Moholkar, A. V., Khot, V. M., & Patil, A. R. (2024). Fabrication of magnetite nanoparticles as a potential photocatalytic agent with cytotoxicity response. *BioNanoscience*, 14(3), 2197-2217.
143. Bhattacharya, S., Bagade, S., Sangave, P. C., Kumar, D., Shaik, I., & Mukherjee, D. (2024). Comparative Study of pH-Responsive and Aggregation Stability of Bosutinib-Loaded Nanogels Comprising Gelatin Methacryloyl, Carboxymethyl Dextran, and Hyaluronic Acid for Controlled Drug Delivery in Colorectal Cancer: An Extensive In Vitro Investigation. *Biomacromolecules*, 25(12), 7926-7950.
144. Wan, X., Zhang, Y., Wan, Y., Xiong, M., Xie, A., Liang, Y., & Wan, H. (2024). A multifunctional biomimetic nanoplatfom for dual tumor targeting-assisted multimodal therapy of colon cancer. *ACS nano*, 18(39), 26666-26689.
145. Tabasi, H., Mosavian, M. H., Sabouri, Z., Khazaei, M., & Darroudi, M. (2021). pH-responsive and CD44-targeting by Fe3O4/MSNs-NH2 nanocarriers for oxaliplatin loading and colon cancer treatment. *Inorganic Chemistry Communications*, 125, 108430.
146. Alfassam, H. E., Al Othman, S. I., Al-Waili, M. A., Allam, A. A., & Abukhadra, M. R. (2023). Characterization of β -cyclodextrin Hybridized Diatomite as Potential Delivery Systems of Oxaliplatin and 5-Fluorouracil Drugs; Equilibrium Modeling of Loading and Release Kinetics. *Journal of Macromolecular Science, Part B*, 62(9), 478-503.
147. Jahedi, M., & Meshkini, A. (2023). Tumor tropic delivery of FU. FA@ NSs using mesenchymal stem cells for synergistic chemo-photodynamic therapy of colorectal cancer. *Colloids and Surfaces B: Biointerfaces*, 226, 113333.
148. Hassan, Y. A., Alfaihi, M. Y., Shati, A. A., Elbehairi, S. E. I., Elshaarawy, R. F., & Kamal, I. (2022). Co-delivery of anticancer drugs via poly (ionic crosslinked chitosan-palladium) nanocapsules: Targeting more effective and sustainable cancer therapy. *Journal of Drug Delivery Science and Technology*, 69, 103151.
149. Feng, H., Li, M., Xing, Z., Ouyang, X. K., & Ling, J. (2022). Efficient delivery of fucoxanthin using metal-polyphenol network-coated magnetic mesoporous silica. *Journal of Drug Delivery Science and Technology*, 77, 103842.
150. Uzun, M. B., Guderer, I., Banerjee, S., & Yilmaz, A. (2025). Synthesis and photoluminescence properties of Ce3+/Tb3+ and Eu3+ ions doped GdB3O6/Ca10 (PO4) 6 (OH) 2 Core/Shell particles as well as its cytotoxicity against colon cancer cells. *Journal of Molecular Structure*, 1321, 139921.
151. Du, J., Liu, J., Zhao, Z., Dai, J., Li, K., & Lin, Y. (2022). Nonmetallic N/C nanozyme performs continuous consumption of glu for inhibition of colorectal cancer cells. *ACS Applied Bio Materials*, 6(1), 267-276.
152. Kumar, B., Kulanthaivel, S., Mondal, A., Mishra, S., Banerjee, B., Bhaumik, A., ... & Giri, S. (2017). Mesoporous silica nanoparticle based enzyme responsive system for colon specific drug delivery through guar gum capping. *Colloids and Surfaces B: Biointerfaces*, 150, 352-361.
153. Mahboubi, F., Mohammadnejad, J., & Khaleghi, S. (2024). Bifunctional folic acid targeted biopolymer Ag@ NMOF nanocomposite [$\{Zn_2(1,4\text{-bdc})_2(\text{DABCO})\}_n$] as a novel theranostic agent for molecular imaging of colon cancer by SERS. *Heliyon*, 10(8).
154. Li, Q., Liu, J., Fan, H., Shi, L., Deng, Y., Zhao, L., ... & Wang, Z. (2021). IDO-inhibitor potentiated immunogenic

- chemotherapy abolishes primary tumor growth and eradicates metastatic lesions by targeting distinct compartments within tumor microenvironment. *Biomaterials*, 269, 120388.
155. Bullo, S., Buskaran, K., Baby, R., Dorniani, D., Fakurazi, S., & Hussein, M. Z. (2019). Dual Drugs Anticancer Nanoformulation using Graphene Oxide-PEG as Nanocarrier for Protocatechuic Acid and Chlorogenic Acid: Bullo et al. *Pharmaceutical research*, 36(6), 91.
156. Ge, D., Ren, D., Duan, Y., Luo, X., He, S., Qin, W., ... & Zhang, C. (2025). Hollow MnO₂-based multifunctional nanoplatform for enhanced tumor chemodynamic therapy. *Science China Materials*, 68(1), 292-302.
157. Jiang, H., Shi, X., Yu, X., He, X., An, Y., & Lu, H. (2018). Hyaluronidase Enzyme-responsive Targeted Nanoparticles for Effective Delivery of 5-Fluorouracil in Colon Cancer: Jiang et al. *Pharmaceutical research*, 35(4), 73.
158. AbouAitah, K., Stefanek, A., Higazy, I. M., Janczewska, M., Swiderska-Sroda, A., Chodara, A., ... & Lojkowski, W. (2020). Effective targeting of colon cancer cells with piperine natural anticancer prodrug using functionalized clusters of hydroxyapatite nanoparticles. *Pharmaceutics*, 12(1), 70.
159. Jin, J., Chen, Y., Li, H., Xu, Y., & Wang, L. (2024). Loading polyaniline (PANI) nanoparticles to mesoporous hydroxyapatite (HAp) spheres for near infrared (NIR) induced doxorubicin (DOX) drug delivery and colon cancer treatment. *Physical Chemistry Chemical Physics*, 26(35), 23277-23287.
160. Guo, J. C., Deng, S. H., Zhou, S. M., Zhou, X., Du, J., Zhou, S. H., ... & Xie, M. J. (2024). Responsive ZIF-90 nanocomposite material: targeted delivery of 10-hydroxycamptothecin to enhance the therapeutic effect of colon cancer (HCT116) cells. *RSC Medicinal Chemistry*, 15(8), 2663-2676.
161. Rayappan, K., Murugan, C., Sundarraj, S., Lara, R. P., & Kannan, S. (2017). Peptide-Conjugated Nano-Drug Delivery System to Improve Synergistic Molecular Chemotherapy for Colon Carcinoma. *ChemistrySelect*, 2(27), 8524-8534.
162. Cai, D., Han, C., Liu, C., Ma, X., Qian, J., Zhou, J., ... & Zhu, W. (2020). Chitosan-capped enzyme-responsive hollow mesoporous silica nanoplatforms for colon-specific drug delivery. *Nanoscale Research Letters*, 15(1), 123.
163. Zhou, H., Yang, J., Li, Z., Feng, J., Duan, X., Yan, C., ... & Shen, Z. (2024). Hollow mesoporous calcium peroxide nanoparticles for drug-free tumor calcicoptosis therapy. *Acta Biomaterialia*, 185, 456-466.
164. Öztürk, A. B., Oğuz, N., Şahin, H. T., Emik, S., & Alarcin, E. (2020). Design of an amphiphilic hyperbranched core/shell-type polymeric nanocarrier platform for drug delivery. *Turkish Journal of Chemistry*, 44(2), 518-534.
165. Xu, H., Su, Z., Zhang, H., Zhang, Y., Bao, Y., Zhang, H., ... & Jin, Y. (2023). Cu²⁺-pyropheophorbide-a-cystine conjugate-mediated multifunctional mesoporous silica nanoparticles for photo-chemodynamic therapy/GSH depletion combined with immunotherapy cancer. *International Journal of Pharmaceutics*, 640, 123002.
166. Tang, J., Chen, Y., Lai, H., Zeng, Q., Li, Y., Feng, J., ... & Liang, Z. (2025). Innovative immunosonogen nanoplatform combining sonodynamic oxygenation and immunomodulation for superior cancer therapy. *Chemical Engineering Journal*, 515, 163582.
167. Zhang, Z., Zhang, L., Huang, C., Guo, Q., Zuo, Y., Wang, N., ... & Zhu, D. (2020). Gas-generating mesoporous silica nanoparticles with rapid localized drug release for enhanced chemophotothermal tumor therapy. *Biomaterials science*, 8(23), 6754-6763.
168. Zhang, J., Fang, R., Song, N., Jin, Y., Zhang, M., Wang, J., ... & Yang, X. (2025). Multifunctional Liposomes with Enhanced Stability for Imaging-Guided Cancer Chemodynamic and Photothermal Therapy. *ACS Biomaterials Science & Engineering*, 11(4), 2146-2156.
169. Meka, A. K., Jenkins, L. J., Dávalos-Salas, M., Pujara, N., Wong, K. Y., Kumeria, T., ... & Popat, A. (2018). Enhanced solubility, permeability and anticancer activity of vorinostat using tailored mesoporous silica nanoparticles. *Pharmaceutics*, 10(4), 283.
170. Summerlin, N., Qu, Z., Pujara, N., Sheng, Y., Jambhrunkar, S., McGuckin, M., & Popat, A. (2016). Colloidal mesoporous silica nanoparticles enhance the biological activity of resveratrol. *Colloids and Surfaces B: Biointerfaces*, 144, 1-7.
171. Shen, Y., Wang, L., Ji, B., Lu, X., Zhao, D., Dai, Y., & Meng, X. (2024). Stimulus-responsive nanomedicine mediated by metabolic intervention mechanisms to amplify redox anticancer therapy. *Chemical Engineering Journal*, 486, 150130.
172. Zarkesh, K., Heidari, R., Iranpour, P., Azarpira, N., Ahmadi, F., Mohammadi-Samani, S., & Farjadian, F. (2022). Theranostic hyaluronan coated EDTA modified magnetic mesoporous silica nanoparticles for targeted delivery of cisplatin. *Journal of Drug Delivery Science and Technology*, 77, 103903.
173. Zhang, D., He, X., Wei, Y., Fan, Q., Qiao, J., Jin, G., & Li, N. (2024). GSH-responsive magnetic mesoporous silica nanoparticles for efficient controlled drug delivery in tumor cells. *AIP Advances*, 14(10).
174. Guo, M., Ling, J., Xu, X., & Ouyang, X. (2023). Delivery of doxorubicin by ferric ion-modified mesoporous polydopamine nanoparticles and anticancer activity against HCT-116 cells in vitro. *International Journal of Molecular Sciences*, 24(7), 6854.
175. Farjadian, F., Moghadam, M., Monfared, M., & Mohammadi-Samani, S. (2022). Mesoporous silica nanostructure modified with azo gatekeepers for colon targeted delivery of 5-fluorouracil. *AIChE Journal*, 68(12), e17900.
176. Alallam, B., Abdkadir, E., Hayati, A., Keong, Y. Y., & Lim, V. (2025). Alginate coated mesoporous silica nanoparticles as oral delivery carrier of curcumin and quercetin to colon cancer: preparation, optimization, characterization, and anticancer activity. *Drug Delivery and Translational Research*, 15(11), 3793-3834.
177. Singh, P., Singh, H., Castro-Aceituno, V., Ahn, S., Kim, Y. J., Farh, M. E. A., & Yang, D. C. (2017). Engineering of mesoporous silica nanoparticles for release of ginsenoside CK and Rh2 to enhance their anticancer and anti-inflammatory

- efficacy: In vitro studies. *Journal of Nanoparticle Research*, 19(7), 257.
178. Andrade, J. D. L., Moreira, C. A., Oliveira, A. G., de Freitas, C. F., Montanha, M. C., Hechenleitner, A. A. W., ... & de Oliveira, D. M. F. (2022). Rice husk-derived mesoporous silica as a promising platform for chemotherapeutic drug delivery. *Waste and biomass valorization*, 13(1), 241-254.
179. Lahmadi, S., Alamery, S., Beagan, A., Alotaibi, K., & Alswieleh, A. (2024). Advanced hybrid silica nanoparticles with pH-responsive diblock copolymer brushes: optimized design for controlled doxorubicin loading and release in cancer therapy. *RSC advances*, 14(13), 8819-8828.
180. Karnopp, J. C. F., Jorge, J., da Silva, J. R., Boldo, D., Del Pino Santos, K. F., Duarte, A. P., ... & Martines, M. A. U. (2024). Synthesis, Characterization, and Cytotoxicity Evaluation of Chlorambucil-Functionalized Mesoporous Silica Nanoparticles. *Pharmaceutics*, 16(8), 1086.
181. AbouAitah, K., Hassan, H. A., Swiderska-Sroda, A., Gohar, L., Shaker, O. G., Wojnarowicz, J., ... & Lojkowski, W. (2020). Targeted nano-drug delivery of colchicine against colon cancer cells by means of mesoporous silica nanoparticles. *Cancers*, 12(1), 144.
182. Shen, J. J., Xue, S. J., Mei, Z. H., Li, T. T., Li, H. F., Zhuang, X. F., & Pan, L. M. (2024). Synthesis, characterization, and efficacy evaluation of a PH-responsive Fe-MOF@ GO composite drug delivery system for the treating colorectal cancer. *Heliyon*, 10(6).
183. Falemban, A. H., Ibrahim, I. A. A., Bamagous, G. A., Alzahrani, A. R., Shahid, I., Shahzad, N., ... & Thangavelu, I. (2025). Fabrication of NiO nanoparticles modified with carboxymethyl cellulose and D-carvone for enhanced antimicrobial, antioxidant and anti-cancer activities. *Inorganic Chemistry Communications*, 171, 113517.
184. Khatibi, Z., Kazemi, N. M., & Khaleghi, S. (2022). Targeted and biocompatible NMOF as efficient nanocomposite for delivery of methotrexate to colon cancer cells. *Journal of Drug Delivery Science and Technology*, 73, 103441.
185. Pei, M., Liu, K., Qu, X., Wang, K., Chen, Q., Zhang, Y., ... & Zhang, Y. (2023). Enzyme-catalyzed synthesis of selenium-doped manganese phosphate for synergistic therapy of drug-resistant colorectal cancer. *Journal of Nanobiotechnology*, 21(1), 72.
186. Ayub, A. D., Chiu, H. I., Mat Yusuf, S. N. A., Abd Kadir, E., Ngalm, S. H., & Lim, V. (2019). Biocompatible disulphide cross-linked sodium alginate derivative nanoparticles for oral colon-targeted drug delivery. *Artificial cells, nanomedicine, and biotechnology*, 47(1), 353-369.
187. Sahoo, P., Kundu, S., Roy, S., Sharma, S. K., Ghosh, J., Mishra, S., ... & Ghosh, C. K. (2022). Fundamental understanding of the size and surface modification effects on r 1, the relaxivity of Prussian blue nanocube@ m-SiO 2: a novel targeted chemo-photodynamic theranostic agent to treat colon cancer. *RSC advances*, 12(38), 24555-24570.
188. Liu, Q., Xiang, Y., Yu, Q., Lv, Q., & Xiang, Z. (2024). A TME-activated nano-catalyst for triple synergistic therapy of colorectal cancer. *Scientific reports*, 14(1), 3328.
189. Singh, H., PonnannEttiyappan, J., & BalaKrishnan, R. (2025). Amidated pectin and gum Arabic aldehyde-based pH-sensitive hydrogel for targeted colonic treatment. *Colloids and Surfaces A: Physicochemical and Engineering Aspects*, 724, 137390.
190. Le, B. T., Nguyen, C. Q., Nguyen, P. T., Ninh, H. D., Le, T. M., Nguyen, P. T. H., & La, D. D. (2022). Fabrication of porous Fe-based metal-organic complex for the enhanced delivery of 5-fluorouracil in in vitro treatment of cancer cells. *ACS omega*, 7(50), 46674-46681.
191. Le, U. C. N., Mai, N. X. D., Le, K. M., Vu, H. A., Tran, H. N. T., & Doan, T. L. H. (2024). Development and evaluation of rosmarinic acid loaded novel fluorescent porous organosilica nanoparticles as potential drug delivery system for cancer treatment. *Arabian Journal of Chemistry*, 17(1), 105402.
192. Foroutan, R., Mohammadzadeh, A., Javanbakht, S., Mohammadi, R., & Ghorbani, M. (2025). Alginate/magnetic hydroxyapatite bio-nanocomposite hydrogel bead as a pH-responsive oral drug carrier for potential colon cancer therapy. *Results in Chemistry*, 15, 102177.
193. Thorat, N. D., Bauer, J., Tofail, S. A., Perez, V. G., Bohara, R. A., & Yadav, H. M. (2020). Silica nano supra-assembly for the targeted delivery of therapeutic cargo to overcome chemoresistance in cancer. *Colloids and Surfaces B: Biointerfaces*, 185, 110571.
194. Abrishami, A., Bahrami, A. R., Saljooghi, A. S., & Matin, M. M. (2024). Enhanced theranostic efficacy of epirubicin-loaded SPION@ MSN through co-delivery of an anti-miR-21-expressing plasmid and ZIF-8 hybridization to target colon adenocarcinoma. *Nanoscale*, 16(12), 6215-6240.
195. Hassanpouraghdam, Y., Pooresmaeil, M., & Namazi, H. (2022). In-vitro evaluation of the 5-fluorouracil loaded GQDs@ Bio-MOF capped with starch biopolymer for improved colon-specific delivery. *International journal of biological macromolecules*, 221, 256-267.
196. Alavinia, S., Ghorbani-Vaghei, R., Haddadi, R., Sanemar, K., Uroomiye, S. S., Nourian, A., & Emami, N. (2025). Anticancer effects of silymarin-loaded ACA-HA/sulfonamide IR-MOF nanoplatform in CT-26 xenograft model. *International Journal of Biological Macromolecules*, 309, 142651.
197. Bhattacharyya, S., Fernandaes, R.I. (2025). An in vitro characterization and cytotoxic evaluation of mesoporous delivery of celecoxib on anticancer activity, *European Journal of Parenteral and Pharmaceutical Sciences*, 301.
198. Qiao, L., Ou, Y., Li, L., Wu, S., Guo, Y., Liu, M., ... & Li, Z. (2024). H2S-driven chemotherapy and mild photothermal therapy induced mitochondrial reprogramming to promote cuproptosis. *Journal of Nanobiotechnology*, 22(1), 205.
199. ghalee-taki, G. N., Rastegari, A. A., Hekmat, A., & Rezaee, M. (2024). Synthesis and Characterization of Zinc Oxide-Chitosan Nanocomposite for Targeted Drug Delivery to the Colon. *BioNanoScience*, 14(3), 2337-2364.
200. Cui, C., Sun, Z., Gao, Y. X., & Sun, Q. (2025). Synthesis of

- microporous silica nanoparticles as a versatile nanocarrier for 5-fluorouracil delivery in colon cancer chemotherapy. *Journal of Nanoparticle Research*, 27(7), 191.
201. Thirumalaivasan, N., Venkatesan, P., Lai, P. S., & Wu, S. P. (2019). In vitro and in vivo approach of hydrogen-sulfide-responsive drug release driven by azide-functionalized mesoporous silica nanoparticles. *ACS Applied Bio Materials*, 2(9), 3886-3896.
202. Li, Y., Zhou, J., Wang, L., & Xie, Z. (2020). Endogenous hydrogen sulfide-triggered MOF-based nanoenzyme for synergic cancer therapy. *ACS applied materials & interfaces*, 12(27), 30213-30220.
203. Iranpour, S., Bahrami, A. R., Nekooei, S., Sh. Saljooghi, A., & Matin, M. M. (2021). Improving anti-cancer drug delivery performance of magnetic mesoporous silica nanocarriers for more efficient colorectal cancer therapy. *Journal of Nanobiotechnology*, 19(1), 314.
204. Mohammadi, R., Saboury, A., Javanbakht, S., Foroutan, R., & Shaabani, A. (2021). Carboxymethylcellulose/polyacrylic acid/starch-modified Fe₃O₄ interpenetrating magnetic nanocomposite hydrogel beads as pH-sensitive carrier for oral anticancer drug delivery system. *European Polymer Journal*, 153, 110500.
205. Vilaça, N., Bertão, A. R., Prasetyanto, E. A., Granja, S., Costa, M., Fernandes, R., ... & Neves, I. C. (2021). Surface functionalization of zeolite-based drug delivery systems enhances their antitumoral activity in vivo. *Materials Science and Engineering: C*, 120, 111721.
206. Parsaei, M., & Akhbari, K. (2022). MOF-801 as a nanoporous water-based carrier system for in situ encapsulation and sustained release of 5-FU for effective cancer therapy. *Inorganic Chemistry*, 61(15), 5912-5925.
207. Liu, W., Wang, F., Zhu, Y., Li, X., Liu, X., Pang, J., & Pan, W. (2018). Galactosylated chitosan-functionalized mesoporous silica nanoparticle loading by calcium leucovorin for colon cancer cell-targeted drug delivery. *Molecules*, 23(12), 3082.
208. Anirudhan, T. S., & Nair, S. S. (2019). Polyelectrolyte complexes of carboxymethyl chitosan/alginate based drug carrier for targeted and controlled release of dual drug. *Journal of Drug Delivery Science and Technology*, 51, 569-582.
209. Babaei, M., Abrishami, A., Iranpour, S., Saljooghi, A. S., & Matin, M. M. (2025). Harnessing curcumin in a multifunctional biodegradable metal-organic framework (bio-MOF) for targeted colorectal cancer theranostics. *Drug Delivery and Translational Research*, 15(5), 1719-1738.
210. Sun, T., Xia, R., Zhou, J., Zheng, X., Liu, S., & Xie, Z. (2020). Protein-assisted synthesis of nanoscale covalent organic frameworks for phototherapy of cancer. *Materials Chemistry Frontiers*, 4(8), 2346-2356.
211. Zhou, Y., Liu, S., Hu, C., Cai, L., & Pang, M. (2020). A covalent organic framework as a nanocarrier for synergistic phototherapy and immunotherapy. *Journal of Materials Chemistry B*, 8(25), 5451-5459.
212. Yamane, S., Yusri, A. H. B., Chen, P. Y., van der Vlies, A. J., Mabrouk, A. B., Fetzter, I., & Hasegawa, U. (2025). Surface Coating of ZIF-8 Nanoparticles with Polyacrylic Acid: A Facile Approach to Enhance Chemical Stability for Biomedical Applications. *Macromolecular Bioscience*, 25(2), 2400382.
213. Dalei, G., Jena, D., & Das, S. (2024). 5-Fluorouracil-loaded green chitosan nanoparticles/guar gum nanocomposite hydrogel in controlled drug delivery. *Carbohydrate Research*, 545, 109257.
214. Jian, X., Xu, J., Yang, L., Zhao, C., Xu, J., Gao, Z., & Song, Y. Y. (2020). Intracellular metal-organic frameworks: Integrating an all-in-one semiconductor electrode chip for therapy, capture, and quantification of circulating tumor cells. *Analytical chemistry*, 92(19), 13319-13326.
215. Hashemzadeh, A., Amerizadeh, F., Asgharzadeh, F., Drummen, G. P., Hassanian, S. M., Landarani, M., ... & Khazaei, M. (2022). Magnetic amine-functionalized UiO-66 for oxaliplatin delivery to colon cancer cells: in vitro studies. *Journal of Cluster Science*, 33(5), 2345-2361.
216. Chen, J., Wang, C., Zhu, Z. Y., Wang, F., Shang, J., Liu, Z., & Wang, L. (2024). Titanium-based metal-organic frameworks as pH-responsive drug delivery carriers of 5-Fluorouracil. *Journal of Solid State Chemistry*, 332, 124563.
217. Liu, C., Jiang, F., Xing, Z., Fan, L., Li, Y., Wang, S., ... & Ouyang, X. K. (2022). Efficient delivery of curcumin by alginate oligosaccharide coated aminated mesoporous silica nanoparticles and in vitro anticancer activity against colon cancer cells. *Pharmaceutics*, 14(6), 1166.
218. Gholami, M., Hekmat, A., Khazaei, M., & Darroudi, M. (2022). OXA-CuS@ UiO-66-NH₂ as a drug delivery system for Oxaliplatin to colorectal cancer cells. *Journal of Materials Science: Materials in Medicine*, 33(3), 26.
219. Tehrani Nejad, S., Rahimi, R., Najafi, M., & Rostamnia, S. (2024). Sustainable gold nanoparticle (Au-NP) growth within interspaces of porphyrinic Zirconium-Based Metal-Organic frameworks: green synthesis of PCN-224/Au-NPs and its anticancer effect on colorectal cancer cells assay. *ACS Applied Materials & Interfaces*, 16(3), 3162-3170.
220. Nabipour, H., & Hu, Y. (2022). Development of fully bio-based pectin/curcumin@ bio-MOF-11 for colon specific drug delivery. *Chemical Papers*, 76(5), 2969-2979.
221. Zhang, W. J., Babu, A., Yan, Y. Z., Park, S. S., Jo, N. J., Chung, I., ... & Ha, C. S. (2023). ROS/GSH dual-responsive selenium-containing mesoporous silica nanoparticles for drug delivery. *Journal of Porous Materials*, 30(5), 1469-1484.
222. Sun, X., Li, F., Yuan, L., Bing, Z., Li, X., & Yang, K. (2024). pH-responsive resveratrol-loaded ZIF-8 nanoparticles modified with tannic acid for promoting colon cancer cell apoptosis. *Journal of Biomedical Materials Research Part B: Applied Biomaterials*, 112(1), e35320.
223. Abd-Elsatar, A. G., Farag, M. M., Youssef, H. F., Salih, S. A., Mounier, M. M., & El-Meliegy, E. (2019). Different zeolite systems for colon cancer therapy: Monitoring of ion release, cytotoxicity and drug release behavior. *Progress in*

-
- biomaterials*, 8(2), 101-113.
224. Nagaraja, K., Rao, K. M., Rao, K. K., & Han, S. S. (2022). Dual responsive tamarind gum-co-poly (N-isopropyl acrylamide-co-ethylene glycol vinyl ether) hydrogel: A promising device for colon specific anti-cancer drug delivery. *Colloids and Surfaces A: Physicochemical and Engineering Aspects*, 641, 128456.
225. Tarasi, S., Ramazani, A., Morsali, A., Hu, M. L., Ghafghazi, S., Tarasi, R., & Ahmadi, Y. (2022). Drug delivery using hydrophilic metal-organic frameworks (MOFs): Effect of structure properties of MOFs on biological behavior of carriers. *Inorganic Chemistry*, 61(33), 13125-13132.
226. Johari, S. A., Sarkheil, M., & Veisi, S. (2021). Cytotoxicity, oxidative stress, and apoptosis in human embryonic kidney (HEK293) and colon cancer (SW480) cell lines exposed to nanoscale zeolitic imidazolate framework 8 (ZIF-8). *Environmental Science and Pollution Research*, 28(40), 56772-56781.
227. Chun, N. Y., Kim, S. N., Choi, Y. S., & Choy, Y. B. (2020). PCN-223 as a drug carrier for potential treatment of colorectal cancer. *Journal of Industrial and Engineering Chemistry*, 84, 290-296.
228. Das, S. K., Mishra, S., Saha, K. D., Chandra, D., Hara, M., Mostafa, A. A., & Bhaumik, A. (2022). N-rich, polyphenolic porous organic polymer and its in vitro anticancer activity on colorectal cancer. *Molecules*, 27(21), 7326.
229. Soroushmanesh, M., Dinari, M., & Jalali, H. (2025). Encapsulation of Irinotecan in nanoporous porphyrin-based COF: An efficient drug delivery system for colorectal and breast cancer treatment. *Results in Engineering*, 27, 105919.

Copyright: ©2026 Sana Tat, et al. This is an open-access article distributed under the terms of the Creative Commons Attribution License, which permits unrestricted use, distribution, and reproduction in any medium, provided the original author and source are credited.